The SUPECA kinetics for scaling redox reactions in networks of mixed substrates and consumers and an example application to aerobic soil respiration

Jinyun Tang and William J. Riley

Earth and Environmental Sciences Area, Lawrence Berkeley National Laboratory, Berkeley, CA, USA, 94720

Correspondence to: J. Y. Tang (jinyuntang@lbl.gov)

Abstract. Several land biogeochemical models used for studying carbon-climate feedbacks have begun explicitly representing microbial processes. However, to our knowledge, there has been no theoretical work on how to achieve a consistent scaling of the complex biogeochemical reactions from microbial individuals to populations, communities, and interactions with plants and mineral soils. We here study this scaling problem by focusing on the substrate-consumer relationships for consumer mediated redox reactions of the form $A+B\xrightarrow{E}products$, where products could be microbial biomass and different bio-products. Under the quasi-steady-state approximation, these substrate-consumer relationships can be formulated as the computationally difficult full Equilibrium Chemistry problem, which is then usually approximated analytically with the popular Dual Monod (DM) kinetics and Synthesizing Unit (SU) kinetics. However, we found that the DM kinetics is scaling inconsistent for reaction networks because it (1) does not incorporate substrate limitation in its derivation, (2) invokes contradictory assumptions regarding the substrate processing rate when transitioning from single substrate reactions to two-substrate redox reactions, and (3) cannot scale the product generation rate from one to multiple substrates. In contrast, the SU kinetics can

consistently scale the product generation rate from one to multiple substrates, but suffers from the deficit that as the consumer abundance approaches infinity, it predicts singular infinite reaction rates even for limited substrates. We attribute this deficit to SU's failure to incorporate the substrate limitation in its derivation and remedy SU with the proposed SUPECA (SU Plus Equilibrium Chemistry Approximation) kinetics, which consistently imposes the mass balance constraints from both substrates and consumers on consumer-substrate interactions in calculating redox reaction rates. Moreover, we show the SUPECA kinetics satisfies the partition principle as in theories like Newton's Law of motion and Dalton's law of partial pressures, such that its mathematical manifestation is scaling invariant when transitioning from an individual reaction to a network of many reactions. We benchmarked the SUPECA kinetics with the equilibrium chemistry solution for some simple problem configurations and found SUPECA outperformed the SU kinetics. In applying the SUPECA kinetics to aerobic soil respiration, we found that SUPECA predicted consistent but variable moisture response functions that agreed well to those derived from incubation data. We finally discuss how the SUPECA kinetics could help Earth System Models consistently incorporate more biogeochemical reactions to improve their biogeochemical modules.

Keywords: Dual-Monod kinetics, Synthesizing Unit, SUPECA kinetics, soil respiration, trait-based modeling

1. Introduction

Land holds more than twice the carbon that is in atmosphere; therefore a small change in land carbon dynamics can imply significant feedbacks to the ongoing climate warming (Ciais et al., 2013). This has motivated intense research towards better understanding of Earth's land biogeochemical cycles, both for prediction and assessing the efficacy of climate mitigation and adaptation strategies. To date, however, soil biogeochemical models are suffering from high uncertainty (e.g., Arora et al., 2013; Bouskill et al. 2014; Friedlingstein et al., 2014; He et al. 2016). For instance, eight CMIP5 Earth System Models (ESMs) predicted that the net land carbon uptake varies from 22 to 456 PgC for the 2006-2100 period under the Representative Concentration Pathway 4.5 (RCP4.5; Shao et al., 2013). Similarly, the 16 CMIP5 ESM simulations analyzed in Todd-Brown et al. (2013) estimated the contemporary global soil carbon stocks ranging from 510 to 3040 PgC to 1 m depth, while the most recent empirical estimation is 1408±154 PgC to 1 m depth and 2060±217 Pg C to 2 m depth (Batjes, 2016). Therefore, it is urgent to improve our models' predictive power.

The predictive power of existing land biogeochemical models is plagued by uncertainties from structural design, numerical implementation, model parameterization, initial conditions, and forcing data (Tang and Zhuang, 2008; Tang et al., 2010; Luo et al., 2015; Wieder et al., 2015a; Blanke et al., 2016; Tang and Riley, 2016). Among them, developing better model structure and formulation has been identified as a priority. One proposed structural improvement is to include explicit microbial processes (Wieder et al., 2015b), which has recently been shown to enable better predictions of global soil carbon stocks (Wieder et al., 2013), priming effects (Sulman et al., 2014), vertical soil carbon

profiles (Riley et al., 2014), and respiratory temperature sensitivity (Tang and Riley, 2015). A second major proposal is to explicitly resolve the ecosystem nutrient cycle, which aligns with the hypothesis that the potential for increasing land ecosystem carbon uptake resulting from the effect of atmospheric CO_2 fertilization could be limited by nutrient availability (Vitousek, 1982; Shi et al., 2015; Wieder et al., 2015c).

A common process that underlies both of these two proposed structural improvements is the substrate-consumer interaction, which is fundamental for modeling microbial decomposition of substrates (Tang and Riley, 2013a; Riley et al., 2014; Le Roux et al., 2016), mineral soil interaction with adsorptive substrates (Tang and Riley, 2015), and plant-microbe competition for nutrients (Zhu et al., 2016a, 2016b, 2017). In soil, because there are many consumers competing for many substrates in different places at different times, the biogeochemical models being developed must be able to scale the many biogeochemical processes consistently across space, time, and processes. Of the three dimensions that call for scaling (Figure 1), scaling across the spatial and temporal dimensions is achieved through spatial and temporal discretization and integration, which has been intensively studied elsewhere (e.g., Kolditz et al., 1998; Mao et al., 2006), so here we study the scaling along the less studied third dimension—process—with a focus on substrate-consumer interactions.

The substrate-consumer relationship is the first step in formulating biogeochemical models, and is formulated with the so-called substrate kinetics that is a function of consumer and substrate abundance under the influence of various environmental factors, such as soil mineralogy, temperature and moisture (see Tang and Riley (2013a) for a review). Since substrate-consumer kinetics only accounts for how

substrates are taken up by organisms, we contend that readers should not misunderstand our discussion of scaling below as an attempt to do ecological aggregation (e.g., Iwasa et al., 1987; 1989). Rather we are presenting a methodology to improve the consistency in formulating the microdynamics for ecological aggregation.

Within a certain homogeneous space-time-process unit in soil (Figure 1), there are generally three types of substrate-consumer relationships: (1) single-substrate Monod type reactions in the form of $A \xrightarrow{E} products$; (2) the two-substrate redox reactions in the form of $A + B \xrightarrow{E} products$, where substrate A and B are called complementary because they both are required to proceed the redox reaction; and (3) the multi-substrate (>2) reactions $\sum_i A_i \xrightarrow{E} products$. The scaling of the single-substrate Monod type reaction has been extensively discussed in Tang and Riley (2013a), and is resolved with the Equilibrium Chemistry Approximation (ECA) kinetics (and more discussion on the ECA kinetics for process scaling will be provided in later sections when discussing the SUPECA kinetics). Further, because many multi-substrate reactions can be separated into a combination of single-substrate reactions and redox-reactions, our discussion below focuses on achieving a consistent kinetic scaling from a single redox reaction to many reactions in a network.

Mathematically, the problem should be addressed with explicit formulation of all kinetic processes using ordinary differential equations accounting for all substrates and consumers (Chellaboina et al., 2009). However, such a formulation would require too many parameters to drive the model and is numerically very difficult to solve because of its multi-temporal scale nature. By making the quasi-steady-state-approximation (QSSA),

i.e., assuming that the product generation from consumer-substrate complex is much slower than the equilibration between consumers, substrates, and consumer-substrate complexes (Briggs and Haldane, 1925; Pedersen et al., 2008), the full kinetic problem is reduced to the simpler Equilibrium Chemistry (EC) form (e.g., Chellaboina et al., 2009). However, the EC form is also usually very difficult to solve numerically. Therefore, analytical approximations to the EC formulation are generally made.

Two classic analytical approximations for modeling redox-reactions are the Dual Monod (DM) kinetics (e.g., Yeh et al., 2001) and Synthesizing Unit (SU) approach (Kooijman, 1998; Brandt et al., 2003). Although both of them are a special case of the EC formulation (Kooijman, 2010; Tang and Riley, 2013a), they make different assumptions of the relative magnitudes of the involved kinetic parameters. For this, Kooijman (2010) has shown that the DM kinetics inevitably requires the dissociation rate to be much larger than the product-generation rate from the consumer-substrate complexes. In contrast, to apply the single-substrate Monod kinetics (Monod, 1949) or Michaelis-Menten (MM) kinetics (Michaelis and Menten, 1913; which is mathematically identical to the empirical Monod kinetics and they two will be used interchangeably hereafter) does not impose this requirement on its parameters. Moreover, in applications to r-K scaling (e.g., Tilman, 1982; Litchman and Klausmeier, 2008), the single-substrate Monod kinetics even requires the product-generation rate to be faster than the dissociation rate of the consumer-substrate complexes. This contrasting requirement on parameters, as we will show later, fails the DM kinetics to achieve a consistent scaling of substrate-consumer interactions for generic biogeochemical modeling.

We define a kinetic formulation to have consistent scaling when the formulated substrate-consumer relationship: (1) can seamlessly transition from a single substrate-consumer pair to a network of many substrate-consumer pairs without changing its mathematical forms (aka the partition principle) and (2) does not predict any singularity over the whole range of substrate and consumer concentrations (aka the non-singular principle which says that the predicted reaction rate won't increase to infinity as the consumer concentration approaches infinity (e.g., Schnell and Maini, 2000; Tang, 2015)). The full kinetics formulation and its EC formulation both satisfy these two criteria, which can be explained using the following example network of consumer-substrate relationships:

$$S_i + E_j \underset{k_{1,ij}^-}{\overset{k_{1,ij}^+}{\leftrightarrow}} E_j S_i \overset{k_{2,ij}^+}{\rightarrow} P_{ij} + E_j \tag{1}$$

where substrate S_i complexes with consumer E_j to form complex $E_j S_i$, which is then degraded into product P_{ij} and the free consumer. In equation (1) (and throughout this study), the forward kinetic parameters are indicated with superscript "+", while the backward kinetic parameters are with superscript "−". Here and below we assume that the units of all variables are consistently defined, and they are only put forward explicitly when it is necessary to resolve an ambiguity.

The full kinetic formulation for the network of equation (1) is:

$$\frac{d\left[S_i\right]}{dt} = -\left[S_i\right]\sum_j \left(k_{1,ij}^+ \left[E_j\right]\right) + \sum_j \left(k_{1,ij}^- \left[E_j S_i\right]\right) \tag{2}$$

$$\frac{d\left[E_jS_i\right]}{dt}=k_{1,ij}^{+}\left[S_i\right]\left[E_j\right]-\left(k_{1,ij}^{-}+k_{2,ij}^{+}\right)\left[E_jS_i\right] \tag{3}$$

$$\frac{d\left[E_j\right]}{dt}=-\left[E_j\right]\sum_i\left(k_{1,ij}^{+}\left[S_i\right]\right)+\sum_i\left(\left(k_{1,ij}^{-}+k_{2,ij}^{+}\right)\left[E_jS_i\right]\right) \tag{4}$$

where, and also throughout this study, we use $\left[x\right]$ to indicate the concentration of x.

That the full kinetic formulation is consistent with the partition principle is manifested in the first summation in equations (2) and (4). Particularly for equation (4), by defining an appropriate mean specific substrate affinity $k_{1,j}^{+}$, the summation $\sum_i\left(k_{1,ij}^{+}\left[S_i\right]\right)$ can be recast into the form $\sum_i k_{1,ij}^{+}\left[S_i\right]=k_{1,j}^{+}\left[S\right]$, in which $\left[S\right]=\sum_i\left[S_i\right]$ resembles Dalton's law of partial pressures (and many other similar relationships in physics, e.g., Newton's second law of motion (Feynman et al., 1963)) and is clearly partition consistent.

Meanwhile, that the full kinetic formulation satisfies the nonsingular principle can be verified by noting that, at any time:

$$\left[S_i\right]+\sum_j\left[E_jS_i\right]=\left[S_i\right]_T \tag{5}$$

and that the consumption of S_i is through the generation of product from $\left[E_jS_i\right]$. Therefore, by combining equations (2), (3), and (5), the overall consumption rate of S_i (i.e., $\sum_j k_{2,ij}^{+}\left[E_jS_i\right]$) is always smaller than $\left[S_i\right]_T\sum_j k_{2,ij}^{+}$.

Since the EC formulation is obtained by applying QSSA to the full kinetic formulation (i.e., $d\left[E_jS_i\right]/dt\approx 0$ for equation (3)), it automatically satisfies the two

criteria for consistent process scaling. However, the Monod kinetics is scaling inconsistent when it is applied, for example, to the single-substrate competition by multiple populations, or to the multi-substrate consumption by a single population. (e.g., Williams, 1973; Schnell and Mendoza, 2000; Tang et al., 2010; Riley et al., 2011, 2014; Allison, 2012; Bouskill et al., 2012; Wieder et al., 2013, 2014). Specifically, the Monod kinetics violates the partition principle, which can be shown from the following inequality:

$$F_j = \left[E_j\right] \sum_i \frac{k_{2,ij}^{+} \left[S_i\right]}{K_{ij} + \left[S_i\right]} \neq \left[E_j\right] \frac{\sum_i k_{2,ij}^{+} \left[S_i\right] / K_{ij}}{1 + \sum_i \left[S_i\right] / K_{ij}} \tag{6}$$

Here F_j describes the uptake of all substrates S_i by population E_j. The left hand side of the inequality is the uptake computed by directly applying the Monod kinetics, while the right hand side of the inequality is by applying the competitive Monod kinetics (e.g., Litchman and Klausmeier, 2008). The inequality (6) is even true when K_{ij} is independent of i. Besides being inconsistent with the partitioning principle, the Monod kinetics also violates the non-singular principle, which can be demonstrated by observing that, as $\left[E_j\right]$ approaches infinity, so does F_j.

For the competitive Monod kinetics on the right hand side of the inequality in equation (6) (e.g., Murdoch, 1973), if all substrates have the same affinity parameter (i.e., $K_j = K_{ij}$), we have the following

$$F_j = \left[E_j\right] \frac{k_{2,j}^{+} \left(\sum_i \left[S_i\right] \right) \Big/ K_j}{1 + \left(\sum_i \left[S_i\right] \right) \Big/ K_j} = \left[E_j\right] \frac{k_{2,j}^{+} \left[S\right] / K_j}{1 + \left[S\right] / K_j} \tag{7}$$

where $\left[S\right] = \sum_i \left[S_i\right]$ designates the total free concentrations of all substrates. Equation (7) therefore suggests that the competitive Monod kinetics satisfies the partition principle for consistent scaling of substrate-consumer relationships. Nevertheless, because the competitive Monod kinetics is linear in $\left[E_j\right]$, like the classic Monod kinetics, it still violates the non-singular principle for consistent scaling.

In Tang (2015) (and also in Borghans et al. (1996), Tang and Riley (2013a)), it was shown that the linear dependence of F_j on $\left[E_j\right]$ as predicted by the Monod kinetics and similarly by the competitive Monod kinetics is due to their failure to impose the substrate mass (or surface area) balance in deriving their mathematical formulations. This problem has been rectified in the Equilibrium Chemistry Approximation kinetics (Tang and Riley, 2013a), which was shown to predict much more accurate parametric sensitivity than the Monod kinetics in comparing with analytical solutions (Tang, 2015). Since the success of all model calibrations rely on the sensitivity of model predicted responses with respect to model parameters (e.g., Wang et al., 2001; Williams et al, 2005; Tang and Zhuang, 2009; van Werkhoven et al., 2009; Qian et al., 2015), ensuring that the substrate kinetics predicts accurate parametric sensitivity is essential for developing robust biogeochemical models.

We therefore ask the question: how should we achieve a consistent scaling from the simplest redox reaction $A+B\xrightarrow{E}products$ (i.e., AB-E type) to a network that mixes many redox reactions and even single substrate Monod-type reactions (a situation found commonly in nature)? Aside from the two criteria (i.e., the partition principle and non-singularity) discussed above, we suggest a third criterion that a consistent scaling of substrate-consumer relationships should be able to seamlessly transition from a single substrate Monod-type reaction to the AB-E type redox reaction without making contradictory assumptions in its theoretical derivation.

In the following, we address the above question by first presenting the step-by-step derivation of the DM kinetics and the SU kinetics from the EC formulation of the redox reaction $A+B\xrightarrow{E}products$. Conceptually, DM kinetics can be viewed as a direct application of chemical kinetics that the reaction rate of substrates A and B over consumer E is determined by the product of A and B's binding probability to E (which in Monod form is $\left[A\right]/\left(K_A+\left[A\right]\right)$ for substrate A, and $\left[B\right]/\left(K_B+\left[B\right]\right)$ for substrate B). Kooijman (1998) was the first to derive the SU kinetics using the queue theory (e.g., Gross et al., 2011) and Brandt et al. (2003) discussed its use for AB-E type redox reactions. The following derivation will stress on exposing the scaling-inconsistencies implied in the DM kinetics and SU kinetics, and, in particular, we will show that DM kinetics cannot be extended for consistent process scaling of the substrate-consumer relationship. We then present the SUPECA kinetics that remedies the inconsistencies of the SU kinetics. We demonstrate the benefits of SUPECA in terms of its numerical accuracy and present an example application of modeling the moisture control of aerobic

soil respiration. Finally, we discuss how one can apply the SUPECA kinetics to trait-based modeling approaches in various biogeochemical systems.

2. Derivation of ECA kinetics for AB-E type redox reaction $A+B\xrightarrow{E}products$

2.1 Governing equations

We schematically represent the enzymatic redox reaction network as

$$\begin{array}{ccccc} E & + A & \underset{k_A^-}{\overset{k_A^+}{\leftrightarrow}} & EA & \\ + & & & + & \\ B & & & B & \\ k_B^- \updownarrow k_B^+ & & & k_B^- \updownarrow k_B^+ & \\ EB & + A & \underset{k_A^-}{\overset{k_A^+}{\leftrightarrow}} & EAB & \xrightarrow{k_2^+} E + P \end{array} \tag{8}$$

where it is assumed that the order of substrates A and B's binding to consumer E does not affect the kinetic coefficients as is done in most modeling studies (e.g., Yeh et al., 2001).

By law of mass action and the total QSSA (tQSSA; e.g., see Borghans et al., 1996; Tang and Riley, 2013a), we have the governing equations (see appendix A for derivations) as follows:

$$\frac{d\left[A\right]_T}{dt} = -k_2^+\left[EAB\right] \tag{9}$$

$$\frac{d\left[B\right]_T}{dt} = -k_2^+\left[EAB\right] \tag{10}$$

$$k_A^+\left[E\right]\left[A\right]+k_B^-\left[EAB\right]=\left(k_A^-+k_B^+\left[B\right]\right)\left[EA\right] \tag{11}$$

$$k_B^+\left[E\right]\left[B\right]+k_A^-\left[EAB\right]=\left(k_B^-+k_A^+\left[A\right]\right)\left[EB\right] \tag{12}$$

$$k_A^+\left[EB\right]\left[A\right]+k_B^+\left[EA\right]\left[B\right]=\left(k_A^-+k_B^-+k_2^+\right)\left[EAB\right] \tag{13}$$

where

$$\left[A\right]_T = \left[A\right] + \left[EA\right] + \left[EAB\right] \tag{14}$$

$$\left[B\right]_T = \left[B\right] + \left[EB\right] + \left[EAB\right] \tag{15}$$

$$\left[E\right]_T = \left[E\right] + \left[EA\right] + \left[EB\right] + \left[EAB\right] \tag{16}$$

The derivation of substrate kinetics is therefore equivalent to solving for $\left[EAB\right]$ from the EC problem defined by equations (11)-(16). However, because this set of equations is non-linear, and no analytical solutions are available (to our knowledge), some linearization is warranted to obtain analytical approximations. And as we describe below, linearization with different assumptions lead respectively to the DM, SU, and SUPECA kinetics.

To avoid confusions for readers that are not familiar with substrate-kinetics, we also note that because obtaining the substrate kinetics is just to solve equations (11)-(16), various production and destruction terms can be added to equations (9) and (10) without affecting our derivation below.

2.2 **Dual Monod kinetics and synthesizing unit kinetics**

One method to linearize equations (11)-(16) is to assume that the concentration of consumer-substrate complexes are so small that the free substrate concentrations are equal to the bulk concentrations (e.g., for substrate A, it holds $\left[A\right]_T = \left[A\right]$). This approach when combined with different assumptions on the relative magnitudes of the kinetic parameters then leads to the popular DM kinetics and the two-substrate SU kinetics.

2.2.1 Dual Monod kinetics

We now derive the DM kinetics. Adopting the equilibrium approximation that the forward binding between consumer and substrate is in rapid equilibrium with the backward dissociation of the consumer-substrate complex (e.g., Michaelis and Menten, 1913; Pyun, 1971), we have the following

$$\left[EA\right]\left[B\right]=\frac{k_B^-}{k_B^+}\left[EAB\right]=K_B\left[EAB\right] \tag{17}$$

$$\left[EB\right]\left[A\right]=\frac{k_A^-}{k_A^+}\left[EAB\right]=K_A\left[EAB\right] \tag{18}$$

which then transforms equations (11) and (12) into

$$\left[E\right]\left[A\right]=\frac{k_A^-}{k_A^+}\left[EA\right]=K_A\left[EA\right] \tag{19}$$

$$\left[E\right]\left[B\right]=\frac{k_B^-}{k_B^+}\left[EB\right]=K_B\left[EB\right] \tag{20}$$

By solving $\left[EAB\right]$ from equations (14)-(16) using equations (17)-(20), we obtain the consumer-substrate complex for the DM kinetics (see Appendix B)

$$\frac{d\left[A\right]_T}{dt}=-k_2^+\left[E\right]_T\frac{\left[A\right]}{K_A+\left[A\right]}\frac{\left[B\right]}{K_B+\left[B\right]} \tag{21}$$

Although as one substrate, e.g., $\left[A\right]$, approaches infinity, equations (21) can be reduced to the classical MM kinetics

$$\frac{d\left[A\right]_T}{dt}=-k_2^+\frac{\left[E\right]_T\left[B\right]}{K_B+\left[B\right]} \tag{22}$$

we note that the half saturation coefficient $K_B = k_B^- / k_B^+$ in equation (22) is different from its usual definition, which should be $K_B = \left(k_2^+ + k_B^-\right) / k_B^+$, if one derives the MM kinetics rigorously starting from a single substrate and single consumer system (e.g., Tang, 2015). For this reason, we assert that the DM kinetics cannot achieve a self-consistent scaling from one-substrate reaction to multiple-substrate reactions. More specifically, by substituting equations (17) and (18) into equation (13), one obtains $k_2^+ = 0$, or at least $k_2^+ \ll \max\left(k_A^-, k_B^-\right)$, which states that the consumer is very inefficient in processing the substrate. However, MM kinetics does not require the dissociation rate to be much higher than the product generation rate from the consumer-substrate complex, i.e. $k_2^+ \ll \max\left(k_A^-, k_B^-\right)$ (e.g., Briggs and Haldane, 1925). Nor do the high dissociation rates of $\left[EA\right]$, $\left[EB\right]$, and $\left[EAB\right]$ favor the consumer's assimilation of substrates under usual substrate concentrations (e.g., Van Slyke and Cullen, 1914), even though a high dissociation rate may possess some theoretical advantage under high substrate concentrations when the consumer is a single enzyme (Reuveni et al., 2014). To the contrary, most existing applications tend to assume $k_2^+ \gg k_A^-$ and $k_2^+ \gg k_B^-$ (e.g., Holling, 1959, 1966; Aksnes and Egge, 1991; Armstrong, 2008; Bonachela et al., 2011), such that $K_B \approx k_2^+ / k_B^+$ for MM kinetics and the r-K selection can be explained (by linking k_2^+ with growth rate, and k_A^+ and k_B^+ with substrate competitive ability; e.g., Litchman and Klausmeier, 2008). Therefore, for biogeochemical modeling, DM and MM (or Monod)

kinetics are based on different assumptions of the kinetic parameters, and the smooth transition from DM to single substrate Monod kinetics is only ostensible.

2.2.2 Synthesizing unit kinetics

In deriving the SU kinetics for the redox reaction network represented in equation (8), consumer E is viewed as a generalized enzyme that generates bio-products by processing substrates *A* and *B*. SU computes the specific reaction rate per unit concentration of E as the product generation rate k_2^+ times the probability that E binds together with both substrates *A* and *B* (which is $\left[EAB\right]/\left[E\right]_T$). Mathematically, SU kinetics requires the sufficient flux condition $k_A^+\left[A\right] \gg k_B^-$ and $k_B^+\left[B\right] \gg k_A^-$ (Kooijman, 2010). Define $\tilde{k}_2^+ = k_A^- + k_B^- + k_2^+$, equations (11)-(13) become

$$k_A^+\left[E\right]\left[A\right] = k_B^+\left[B\right]\left[EA\right] \tag{23}$$

$$k_B^+\left[E\right]\left[B\right] = k_A^+\left[A\right]\left[EB\right] \tag{24}$$

$$k_A^+\left[EB\right]\left[A\right] + k_B^+\left[EA\right]\left[B\right] = \tilde{k}_2^+\left[EAB\right] \tag{25}$$

From equations (23)-(25), we obtain (see Appendix C)

$$\frac{d\left[A\right]_T}{dt} = -\frac{k_2^+\left[E\right]_T/\tilde{k}_2^+}{\frac{1}{\tilde{k}_2^+} + \frac{1}{k_A^+\left[A\right]} + \frac{1}{k_A^+\left[B\right]} - \frac{1}{k_A^+\left[A\right] + k_A^+\left[B\right]}} \tag{26}$$

The two-substrate SU kinetics as indicated by equation (26) can be viewed alternatively as a special case of the general SU kinetics for any number of complementary substrates, which was derived by Kooijman (1998) based on the queue theory (e.g., Gross et al., 2011). Kooijman (1998) assumed that the consumers act like

synthesizing units, which process the substrates in two steps: binding and production. He then assumed that all flux rates (including production rates k_2^+ and substrate binding rates $k_A^+[A]$ and $k_B^+[B]$) are of Poisson distributions, and calculated the overall specific substrate consumption rate as the reciprocal of the expected total processing time (i.e., the denominator of equation (26)). The last term in the denominator of equation (26) comes from the assumption of parallel binding of substrates A and B to E, and it disappears if sequential binding is assumed.

As one substrate, e.g., A, approaches infinity, the single-substrate Monod kinetics is recovered from equation (26):

$$\frac{d[A]_T}{dt} = -\frac{k_2^+[E]_T}{1+\frac{\tilde{k}_2^+}{k_B^+[B]}} = -\frac{k_2^+[E]_T[B]}{\frac{\tilde{k}_2^+}{k_B^+}+[B]} \tag{27}$$

which has a half saturation coefficient similar to what would be derived for a single substrate, single consumer reaction (e.g., Tang, 2015). By assuming Poisson distribution of the kinetic parameters, it can also be shown for a single enzyme molecule that MM kinetics represents the statistical mean of the fluctuating activity of the enzyme (English et al., 2006; Reuveni et al., 2014). That the kinetics of both single-substrate reaction and two-substrate redox reaction can be similarly derived using statistical theory and that equations (26) and (27) could be obtained from EC formulation using consistent assumptions of the kinetic parameters indicate, in contrast to DM kinetics, that SU kinetics is able to scale consistently between one-substrate and two-substrate redox reactions.

2.3. SUPECA kinetics

In Tang (2015), it was shown that the derivation of MM kinetics ignores the mass balance constraint of substrate, resulting in the MM kinetics to predict inaccurate parametric sensitivity over the wide range of substrate to consumer ratios (e.g., Figure 1 in Tang (2015)). In the above, we also noticed that the substrates mass balance constraints as indicated by equations (14) and (15) are not used in deriving the DM and SU kinetics, suggesting that both the DM and SU kinetics may suffer from the same deficit as the MM kinetics. Further, since the DM kinetics fails to consistently scale from a single substrate to two complementary substrates, we below only remedy the SU kinetics into the SUPECA kinetics to achieve a scalable and non-singular formulation of the redox reactions.

As implied in equations (9)-(16), the derivation of substrate kinetics requires solving for $\left[EAB\right]$ from nonlinear equations (11)-(16), whose analytical solutions are not available. To obtain improved solutions as compared to SU kinetics, we applied a first order closure approach (appendix D; which is the perturbation method truncated to the first order accuracy that describes the first order term using appropriate mean states (e.g., Shankar, 1994; Tang et al., 2007)) to the system formed by equations (11)-(16), leading to the SUPECA kinetics:

$$\frac{d\left[A\right]_T}{dt} = -\frac{\left[E\right]_T}{\frac{1}{k_2^+}\frac{\overline{f}_A\overline{f}_B f_{AB}}{f_A f_B \overline{f}_{AB}} + \frac{1}{f_A} + \frac{1}{f_B} - \frac{f_A\overline{f}_B + \overline{f}_A f_B - \overline{f}_A\overline{f}_B}{f_A f_B \overline{f}_{AB}}} = -\frac{k_2^+\left[E\right]_T\left(f_A/k_2^+\right)\left(f_B/k_2^+\right)}{\frac{\overline{f}_A\overline{f}_B}{k_2^+\overline{f}_{AB}}\frac{f_{AB}}{k_2^+} + \frac{f_{AB}}{k_2^+} - \frac{f_A\overline{f}_B + \overline{f}_A f_B - \overline{f}_A\overline{f}_B}{k_2^+\overline{f}_{AB}}} \tag{28}$$

where $f_A = k_A^+\left[A\right]_T$, $f_B = k_B^+\left[B\right]_T$, $\overline{f}_A = f_A + k_A^+\left[E\right]_T$, $\overline{f}_B = f_B + k_B^+\left[E\right]_T$, $f_{AB} = f_A + f_B$, and $\overline{f}_{AB} = \overline{f}_A + \overline{f}_B$. In equation (28), we assumed $k_2^+ \gg k_A^-$ and $k_2^+ \gg k_B^-$, so that $k_2^+ \approx \tilde{k}_2^+$ (we note that this relationship will be used throughout the remainder of this paper). It can then be verified that if $\left[E\right]_T \ll \left[A\right]_T$ and $\left[E\right]_T \ll \left[B\right]_T$, the SUPECA kinetics as represented in equation (28) becomes the SU kinetics in equation (26). Further, if one of the two substrates, say $\left[B\right]_T$, approaches infinity, equation (28) is reduced to

$$\frac{d\left[A\right]_T}{dt} = -\frac{\left[E\right]_T}{\frac{1}{k_2^+}\frac{\overline{f}_A}{f_A} + \frac{1}{f_A}} = -\frac{f_A\left[E\right]_T}{1 + \frac{\overline{f}_A}{k_2^+}} \tag{29}$$

which by using the definition of f_A and $\overline{f}_A$ can be reduced to the single substrate ECA kinetics equation (Tang, 2015).

3. SUPECA kinetics for a network of reactions

In actual biogeochemical systems, it is more common for many substrates to be processed by many consumers concurrently (and such an assumption is implicitly assumed in the space-time-process unit of any biogeochemical model). To consistently

handle such situations, Tang and Riley (2013a) derived the ECA kinetics (see Figure 2 for a graphic demonstration) for calculating the consumption of a substrate S_i by a consumer E_j in a network of single substrate reactions $A \xrightarrow{E} products$ as

$$\frac{d\left[S_i\right]_{T,j}}{dt} = -\frac{k_{2,ij}^{+}\left[E_j\right]_T\left(\left[S_i\right]_T / K_{ij}\right)}{1+\sum_{l=1}^{l=I}\left(\left[S_l\right]_T / K_{lj}\right)+\sum_{l=1}^{l=J}\left(\left[E_l\right]_T / K_{il}\right)} \tag{30}$$

By defining the normalized substrate flux (with subscript "c" designating that the summation is over a column of the graph in Figure 2)

$$F_{c,j} = \sum_{l=1}^{l=I}\left(\left[S_l\right]_T / K_{lj}\right) = \sum_{l=1}^{l=I} F_{c,j}^{\{l\}} \tag{31}$$

and its conjugate (with subscript "r" designating that the summation is over a row of the graph in Figure 2)

$$F_{r,i} = \sum_{l=1}^{l=J}\left(\left[E_l\right]_T / K_{il}\right) = \sum_{l=1}^{l=J} F_{r,i}^{\{l\}} \tag{32}$$

equation (30) can then be rewritten as

$$\frac{d\left[S_i\right]_{T,j}}{dt} = -k_{2,ij}^{+}\left[E_j\right]_T\left(\frac{F_{c,j}^{\{i\}}}{1+F_{r,i}+F_{c,j}}\right) = -k_{2,ij}^{+}\left[S_i\right]_T\left(\frac{F_{r,i}^{\{j\}}}{1+F_{r,i}+F_{c,j}}\right) \tag{33}$$

The normalized substrate flux as defined in equation (31) and its conjugate in equation (32) implies that the consumption of substrate S_i by consumer E_j as described by the ECA kinetics in equation (33) may be interpreted as either (i) the potential substrate

processing rate of E_j (aka $k_{2,ij}^{+}\left[E_j\right]$) weighted by the relevant importance of the reaction pathway $S_i \xrightarrow{E_j} products$ (aka $F_{c,j}^{\{i\}}$) under the influence of all competing substrate fluxes $F_{c,j}^{\{l\}}$ (towards consumer E_j) and all competing agents' efforts $F_{r,i}^{\{l\}}$ (towards substrate S_i) or (ii) the linear decay potential of S_i (aka $k_{2,ij}^{+}\left[S_i\right]_T$) weighted by relevant importance of $F_{r,i}^{\{j\}}$ under the influence of all competing substrate fluxes and competing agents' efforts.

We further note that equations (31) and (32) define some very interesting scaling relationships. For instance, from equation (31), we can define the effective substrate affinity for the bulk substrates ($\left[\overline{S}\right]_T$ defined as the total of all substrates) that are accessible for consumer E_j as

$$K_{E,j} = \left(\sum_{l=1}^{l=I}\left[S_l\right]_T\right) \Big/ F_{c,j} = \left[\overline{S}\right]_T \Big/ F_{c,j} \tag{34}$$

Similarly, we can define the effective affinity for substrate S_i resulting from all competing agents as

$$K_{S,i} = \left(\sum_{l=1}^{l=J}\left[E_l\right]_T\right) \Big/ F_{r,i} = \left[\overline{E}\right]_T \Big/ F_{r,i} \tag{35}$$

Then by substituting equations (34) and (35) into equation (33), we obtain

$$\frac{d\left[S_i\right]_{T,j}}{dt}=-\frac{k_{2,ij}^{+}\left[E_j\right]_T\left(\left[\bar{S}\right]_T/K_{E,j}\right)}{1+\left[\bar{S}\right]_T/K_{E,j}+\left[\bar{E}\right]_T/K_{S,i}}\frac{F_{c,j}^{\{i\}}}{F_{c,j}}$$
$$=-\frac{k_{2,ij}^{+}\left[S_i\right]_T\left(\left[\bar{E}\right]_T/K_{S,i}\right)}{1+\left[\bar{S}\right]_T/K_{E,j}+\left[\bar{E}\right]_T/K_{S,i}}\frac{F_{r,i}^{\{j\}}}{F_{r,i}} \tag{36}$$

1 which again shows the linear partition in terms of $F_{c,j}^{\{i\}}/F_{c,j}$ and $F_{r,i}^{\{j\}}/F_{r,i}$.

2 By applying the above two scaling relationships and the three consistent scaling
3 criteria (as we proposed in the introduction section) to the SUPECA kinetics in equation
4 (28), we obtain (in appendix E) the network form of the SUPECA kinetics below,

$$\frac{d\left[A_i\right]_{T,jk}}{dt}=-\frac{k_{2,ijk}^{+}\left[E_k\right]_T F_{c,A,k}^{\{i\}}F_{c,B,k}^{\{j\}}}{\frac{G_{A,ik}G_{B,jk}}{G_{AB,ijk}}F_{c,AB,k}+F_{c,AB,k}-\frac{F_{c,A,k}G_{B,jk}+G_{A,ik}F_{c,B,k}-G_{A,ik}G_{B,jk}}{G_{AB,ijk}}} \tag{37}$$

5 where

$$F_{c,A,k}=\sum_l F_{c,A,k}^{\{l\}}=\sum_l\left[A_l\right]_T/K_{A,lk} \tag{38}$$

$$F_{c,B,k}=\sum_l F_{c,B,k}^{\{l\}}=\sum_l\left[B_l\right]_T/K_{B,lk} \tag{39}$$

$$F_{c,AB,k}=F_{c,A,k}+F_{c,B,k} \tag{40}$$

$$F_{r,A,i}=\sum_l\left[E_l\right]_T/K_{A,il} \tag{41}$$

$$F_{r,B,j}=\sum_l\left[E_l\right]_T/K_{B,jl} \tag{42}$$

$$G_{A,ik} = F_{c,A,k} + F_{r,A,i} \tag{43}$$

$$G_{B,jk} = F_{c,B,k} + F_{r,B,j} \tag{44}$$

$$G_{AB,ijk} = G_{A,ik} + G_{B,jk} \tag{45}$$

For equation (37), it is straightforward to verify that if $F_{c,B,k}$ (or $F_{c,A,k}$) goes to infinity, then SUPECA kinetics is reduced to the ECA kinetics in equation (33). Therefore, the SUPECA kinetics as formulated in equation (37) is an extension of both the SU and ECA kinetics, and SUPECA is applicable for consistent scaling of substrate-consumer networks involving both single-substrate reactions and redox-reactions (a visually more appealing demonstration of the SUPECA kinetics is in Figure 3).

4. Accuracy of the SUPECA kinetics

Following Tang and Riley (2013a), we below evaluate the numerical accuracy of the SUPECA kinetics by comparing its solution against that obtained from solving the equilibrium chemistry problem. However, because of numerical complexity, we restricted the comparison to the AB-E problem as formulated by equations (11)-(16) with the assumption of $k_A^- = k_B^- = 0$ and include a substrate sorbent to mimic a class of biogeochemistry problems in soil, such as aerobic soil ammonium nitrification and aerobic soil organic carbon decomposition (formulated in appendix F).

We evaluated the accuracy of SUPECA (equation (37)) and SU (equation (26)) over a wide range of parameter values. Specifically, we fixed both substrates at a nominal

value of 40 mol m^{-3}, and the maximum substrate processing rate at 48 s^{-1}. Then we sampled the affinity parameters exponentially over the range of $[0,1000]$ mol m^{-3} and the microbe and sorbent concentrations uniformly over the range of $[0,1000]$ mol m^{-3}. With a total of 1000 sets of randomly paired parameters, we compared how close the SUPECA and SU approximations are to the EC solution in terms of root mean square error (RMSE) and goodness of linear fit. Because the SU kinetics does not allow a direct integration of the Langmuir adsorption into the calculation of microbe-substrate complexes, we followed Resat et al. (2011) and first solved the Langmuir isotherm to obtain the free substrate concentrations and then entered these free substrate concentrations into SU to obtain the microbe-substrate complex. Apparently, such an artificial ordering in calculation (as needed by the SU approach) suggests that the implementation of SU is numerically cumbersome (and similar numerical difficulties are also associated with the popular MM kinetics (Resat et al., 2011; Tang and Riley, 2013a)).

Our comparison (Figure 4) clearly indicates that the SUPECA kinetics is superior to the SU kinetics in computing the microbe-substrate complex in presence of the substrate binding competition between microbes and sorbent. The SUPECA kinetics is more accurate in terms of both goodness of linear fitting and RMSE. In magnitude, the RMSE of SUPECA predictions is less than 10% of that of SU calculations. The slope of linear fitting from SUPECA calculations is also much closer to the ideal value 1.0, whereas that from SU calculations is far greater than 1.0, suggesting that SU kinetics significantly overestimates microbe-substrate complexes under a wide range of

conditions. This very large slope from SU calculations is also consistent with the singularity at infinite microbial abundances as implied by the linear dependence on microbial abundances in deriving the SU kinetics (equation (26)). Therefore, combined with the better numerical performance of ECA (Tang and Riley, 2013a; Tang, 2015) than MM kinetics, we contend that SUPECA kinetics is both numerically more convenient and more accurate than SU kinetics (which becomes the MM kinetics for one-substrate reactions; see equation (27)) in calculating the microbe-substrate complexes for situations involving microbes, enzymes, substrates and soil minerals (e.g., Tang and Riley, 2015).

5. Example application to modeling aerobic heterotrophic respiration

As an example application, we applied the SUPECA kinetics to model the moisture stress on aerobic soil respiration. In our formulation of the problem (Appendix G), we consider a homogenous 10 cm thick soil with 2.0 mol C m^{-3} microbes and 3.0 mol C m^{-3} dissolvable organic carbon (different DOC values affected our results negligibly as long as they are larger than 0.5 mol C m^{-3}) uniformly distributed across the soil pores. We conceptualize the transport of substrates (i.e., oxygen and DOC) in soil as a two-stage diffusion process (e.g., Grant, 1991) with the first stage from the bulk soil matrix to the water film covering the microbial microsites and the second stage from the water film to the microbial transporters where the substrates are processed. The diffusion processes in soil are calculated based on soil moisture status and the hydraulic properties of a hypothesized soil with a texture of 40% clay and 30% sand. The pedotransfer functions used for calculating soil hydraulic properties are from CLM4.5 (Oleson et al., 2013).

Our conceptual model assumes that the inter microsites (or aggregates) transport dominates the intra-aggregate transport, which is consistent with pore scale simulations (Yang et al., 2014). The model is solved to steady state by assuming that the microbes, atmospheric oxygen, and DOC are in balance under the influence of Langmuir type DOC sorption by soil minerals. Calculations are conducted for three levels of soil minerals (with adsorption capacities at 0, 90, and 180 mol C m^{-3}) and two levels of microbial oxygen affinity (with default $K_{O2,w} = 3 \times 10^{-5}$ mol m^{-3} and elevated $K_{O2,w} = 3 \times 10^{-2}$ mol m^{-3}; Figure 5, Figure 6 and Figure 7). The calculation with elevated $K_{O2,w}$ (when compared to the default $K_{O2,w}$) indicates the effect of soil aggregates on determining microbes' moisture response (see explanations below and in Appendix G). We evaluated (1) how close our predicted moisture response function is to the incubation data from Franzluebbers (1999) and (2) how soil mineral adsorption of DOC would affect the shape of the soil moisture response function.

When the respiration curves are normalized to the range of $[0,1]$, we found that all curves have the pattern that soil respiration first increases from dry soil with increasing moisture and then levels off after reaching a peak value (where the respiration is co-limited by oxygen and DOC bioavailability). The curve with the highest mineral soil carbon adsorption capacity (180 mol C m^{-3}) and elevated $K_{O2,w}$ value best approximates the incubation data from Franzluebbers (1999) and as the sorption capacity becomes smaller, the sharper the moisture response function becomes.

When the affinity parameter of oxygen is reduced to its default value (while keeping the adsorption capacity to 180 mol C m^{-3}; see explanation in Appendix G), the soil moisture response function becomes the sharpest with the highest threshold moisture where the respiration peaks (see green line in Figure 5). Unlike Kausch and Pallud (2013) and Yang et al. (2014), we here have not explicitly prognosed the oxygen distribution inside the aggregates. Since the apparent oxygen affinity parameter (which we use here) generally increases with aggregate size (Griffin, 1968), the poorer agreement of the data with respect to the prediction using the default oxygen affinity parameter indicates that soil aggregates may play an important role in controlling microbes' response to soil moisture stress. Indeed, Franzluebbers (1999) indicated in his Figure 1 that there are significant amount of aggregates in his incubated soil. Moreover, the higher moisture threshold (where respiration peaks) with the default apparent oxygen affinity parameter is also consistent with measurements that aggregates may facilitate anaerobic processes under well-ventilated conditions (by increasing the range of soil moisture conditions where oxygen limits aerobic processes; Renault and Stengel, 1994).

When the effect of different mineral soil carbon adsorption capacity is evaluated against the normalized respiration (Figure 6), we found, being consistent with results described in Tang and Riley (2015), that higher adsorption capacity results in significantly lower soil respiration. Therefore, when the results from Figure 5 and Figure 6 are taken together, we contend that, like the soil temperature effect discussed in Tang and Riley (2015), the soil moisture response function is an emergent response resulting from the interactions between biotic and abiotic factors that co-regulate soil organic carbon decomposition (Manzoni et al., 2016). Such a result strongly contrasts with the

popular approach in existing soil BGC models (e.g., Koven et al., 2013; Tang et al., 2013), which apply a soil moisture response function as a multiplier on an unstressed rate. We therefore suspect that treating moisture stress as a multiplier in modeling soil C decomposition could also significantly bias existing soil biogeochemical model predictions. We will explore such biases in other studies.

When the default oxygen affinity parameter was used in analyzing the effects of different mineral soil carbon adsorption capacities, all the respiration moisture response functions are essentially the same (Figure 7). Since the oxygen affinity parameter reflects the impacts of aggregates at the cm^3 scale, Figures 6 and 7 demonstrate that soil aggregates may have profound influence on soil carbon decomposition rates.

6. Potential applications of the SUPECA kinetics for trait-based biogeochemical modeling

Besides the example application above, we expect that the SUPECA kinetics will be a unique and powerful tool for trait-based modeling in various biogeochemical systems. As we show above and below, the SUPECA kinetics will enable more robust predictions with better numerical consistency and smaller parametric sensitivities than the popular family of Monod kinetics, and SUPECA will be applicable for any biogeochemical system that involves substrate-consumer binding and binding competition.

The assertion of smaller parametric sensitivity as predicted by SUPECA (than by Monod kinetics) can be verified using the single-substrate reaction network as an example. In this case, SUPECA is reduced to ECA kinetics, and for some substrate S_i in

the reaction network, ECA kinetics predicts the sensitivity of its consumption by consumer $\left[E_j\right]$ with respect to the maximum processing rate $k_{2,ij}^{+}$ as

$$\left|\frac{\partial}{\partial k_{2,ij}^{+}}\left(\frac{d\left[S_i\right]_{T,j}}{dt}\right)\right| = \frac{\left[E_j\right]_T F_{c,j}^{\{i\}}}{1+F_{r,i}+F_{c,j}} < \frac{\left[E_j\right]_T F_{c,j}^{\{i\}}}{1+F_{c,j}} < \frac{\left[E_j\right]_T F_{c,j}^{\{i\}}}{1+F_{c,j}^{\{i\}}} \tag{46}$$

where the term after the first "<" is prediction by the competitive Monod kinetics and that after the second "<" is by the Monod kinetics, suggesting that models using Monod kinetics for substrate competition is most sensitive to parameters and least robust to calibrate (e.g., Tang and Riley, 2013a).

To quantitatively evaluate our assertion that SUPECA kinetics predicts lower parametric sensitivity, we, for instance, apply equation (46) to 100 competing substrate fluxes of equal magnitude. We then have $F_{c,j}=100F_{c,j}^{\{i\}}$. Meanwhile, if $F_{c,j}^{\{i\}}>1$, then the sensitivity predicted by competitive Monod kinetics is less than 1% of that by Monod kinetics. Further, if the competing efforts from all agents is comparable to the overall substrate fluxes, i.e., $F_{r,i}\approx F_{c,j}$, then the parametric sensitivity predicted by ECA is about 50% of that by competitive Monod kinetics. Therefore, the ECA (and by extension, SUPECA) prediction is much less sensitive with respect to $k_{2,ij}^{+}$ than that predicted by competitive Monod kinetics and Monod kinetics. Moreover, with equations (30) and (37), one can verify that the more substrates and consumers are represented in the system, the smaller the parametric sensitivity will be predicted by the ECA (and SUPECA) kinetics. One can also verify that such robustness is true for other parameters in the SUPECA kinetics, including the substrates and consumer abundances. That including more

substrates and consumers will leads to more robust model predictions is the fundamental premise that underlines the proposal of trait-based modeling (e.g., Bouskill et al., 2012), and SUPECA is the only kinetics that explicitly contains this presumption in its formulation.

The assertion of wide applicability with SUPECA kinetics has been demonstrated by a number of successful applications that we have published with the ECA kinetics. In a series of studies (Zhu and Riley, 2015; Zhu et al., 2016a, 2016b, 2017), we show that ECA kinetics was able to significantly improve the modeling of nutrient competition between plants, microbes, and mineral soils. In Tang and Riley (2013a), where the ECA kinetics was first proposed, the lignin decomposition dynamics was correctly captured without *a priori* imposing a target lignocellulose index. In Tang and Riley (2013a, 2015) and this study, the ECA kinetics was able to seamlessly incorporate the Langmuir type substrate adsorption into its numerical implementation without invoking the ad hoc numerical order that is prerequisite to MM (or Monod) kinetics for modeling mineral, microbe, and substrate interactions.

Finally, we expect the SUPECA kinetics will provide a robust approach to resolve the redox ladder in soil biogeochemistry. Existing approaches have imposed the redox ladder rigorously following some specific order, e.g. $O_2\ (H_2O)$, $NO_3^-\ (N_2)$, $MnO_2(Mn^{2+})$, $Fe(OH)_3(Fe^{2+})$, $SO_4^{2-}(H_2S)$, $CO_2(CH_4)$, and $H_2O\ (H_2)$ (e.g., Grant, 2001). In contrast, the SUPECA kinetics will allow all these redox-couples to operate concurrently (in any space-time-process unit), a situation that is more consistent with natural soils. Such a feature will also allow the microbial

biogeochemistry models (most of which are considered to be valid at pore scale) to be valid at the scale of well-mixed bulk soils (~cm^3). We are now building such a model and will describe it elsewhere.

7. Conclusion

In this study, we showed that the popular Monod family kinetics and synthesizing unit (SU) kinetics are not scaling consistent for a reaction network involving mixed $A \xrightarrow{E} products$ type and $A+B \xrightarrow{E} products$ type reactions. The SUPECA kinetics, by properly accounting for mass balance constraints of both substrates and consumers, is able to scale such reaction networks without changing its mathematical formulation. Our numerical tests indicate that SUPECA kinetics is superior to SU kinetics both in numerical accuracy and numerical robustness and SUPECA kinetics is able to satisfyingly predict the moisture response function of aerobic soil respiration. Moreover, because SUPECA kinetics intrinsically represents specific microbial traits that can be measured, we expect many more novel modeling applications will be plausible to improve predictions of a wide range of biogeochemical systems.

8. Code and data availability

The source code and data used in this manuscript are available upon request to the corresponding author.

Appendix A: Deriving the governing equations

The law of mass action formulation of the redox reaction (8) is

$$\frac{d[EA]}{dt} = k_A^+[E][A] + k_B^-[EAB] - \left(k_A^- + k_B^+[B]\right)[EA] \quad \text{(A1)}$$

$$\frac{d[EB]}{dt} = k_B^+[E][B] + k_A^-[EAB] - \left(k_B^- + k_A^+[A]\right)[EB] \quad \text{(A2)}$$

$$\frac{d[EAB]}{dt} = k_A^+[EB][A] + k_B^+[EA][B] - \left(k_A^- + k_B^- + k_2^+\right)[EAB] \quad \text{(A3)}$$

$$\frac{d[P]}{dt} = k_2^+[EAB] \quad \text{(A4)}$$

$$\frac{d[A]}{dt} = -k_A^+\left([E] + [EB]\right)[A] + k_A^-\left([EA] + [EAB]\right) \quad \text{(A5)}$$

$$\frac{d[B]}{dt} = -k_B^+\left([E] + [EA]\right)[B] + k_B^-\left([EB] + [EAB]\right) \quad \text{(A6)}$$

We now apply the total quasi-steady-state approximation (e.g., Borghans et al., 1996) to obtain the Equilibrium Chemistry formulation of the system. Specifically, we obtain equations (11)-(13) by respectively setting the time derivatives of equations (A1)-(A3) to zero. Equation (9) is obtained by adding together equations (A1), (A3) and (A5), and using the definition of $[A]_T$ by equation (14). Equation (10) is obtained by adding together equations (A2), (A3) and (A6) with the definition of $[B]_T$ by equation (15).

Appendix B: Deriving the dual Monod kinetics in equation (21)**.**

Replacing $[EA]$ in equation (17) with that obtained from equation (19), we obtain

$$[EAB] = \frac{[A]}{K_A}\frac{[B]}{K_B}[E] \quad \text{(B-1)}$$

By solving $\left[EA\right]$ from equation (19), $\left[EB\right]$ from equation (20) and combining these with equation (B-1) into equation (16), we find

$$\left[E\right]_T = \left(1+\frac{\left[A\right]}{K_A}\right)\left(1+\frac{\left[B\right]}{K_B}\right)\left[E\right] \tag{B-2}$$

Now solve $\left[E\right]$ from (B-2) and enter the result into equation (B-1), we then get

$$\left[EAB\right] = \left(\frac{\left[A\right]}{K_A+\left[A\right]}\right)\left(\frac{\left[B\right]}{K_A+\left[B\right]}\right)\left[E\right]_T \tag{B-3}$$

We thence obtain the dual Monod kinetics by entering equation (B-3) into equation (9).

Appendix C: Deriving the synthesizing unit kinetics in equation (26)

Since SU kinetics assumes that substrates are not limiting the biogeochemical reaction, we then, from equations (23) and (24), obtain

$$\left[EA\right] = \frac{k_A^+\left[A\right]}{k_B^+\left[B\right]}\left[E\right] \tag{C-1}$$

$$\left[EB\right] = \frac{k_B^+\left[B\right]}{k_A^+\left[A\right]}\left[E\right] \tag{C-2}$$

By entering equations (C-1) and (C-2) into equation (13), and solving for $\left[EAB\right]$, we find

$$\left[EAB\right] = \frac{\left[E\right]}{k_2^+ + k_A^- + k_B^-}\left(k_A^+\left[A\right]+k_B^+\left[B\right]\right) = \frac{\left[E\right]}{\tilde{k}_2^+}\left(k_A^+\left[A\right]+k_B^+\left[B\right]\right) \tag{C-3}$$

Now if we combine equations (C-1)-(C-3) with equation (16), we get

$$\left[E\right]=\frac{\left[E\right]_T}{1+\frac{k_A^+\left[A\right]}{k_B^+\left[B\right]}+\frac{k_B^+\left[B\right]}{k_A^+\left[A\right]}+\frac{k_A^+\left[A\right]+k_B^+\left[B\right]}{\tilde{k}_2^+}}$$
$$=\frac{\left[E\right]_T}{\frac{\left(k_A^+\left[A\right]+k_B^+\left[B\right]\right)^2}{\left(k_A^+\left[A\right]\right)\left(k_B^+\left[B\right]\right)}+\frac{k_A^+\left[A\right]+k_B^+\left[B\right]}{\tilde{k}_2^+}-1} \quad \text{(C-4)}$$

which, when combined with equation (C-3), leads to

$$\left[EAB\right]=\frac{k_A^+\left[A\right]+k_B^+\left[B\right]}{\tilde{k}_2^+}\frac{\left[E\right]_T}{\frac{\left(k_A^+\left[A\right]+k_B^+\left[B\right]\right)^2}{\left(k_A^+\left[A\right]\right)\left(k_B^+\left[B\right]\right)}+\frac{k_A^+\left[A\right]+k_B^+\left[B\right]}{\tilde{k}_2^+}-1}$$
$$=\frac{\left[E\right]_T/\tilde{k}_2^+}{\frac{1}{\tilde{k}_2^+}+\frac{k_A^+\left[A\right]+k_B^+\left[B\right]}{\left(k_A^+\left[A\right]\right)\left(k_B^+\left[B\right]\right)}-\frac{1}{k_A^+\left[A\right]+k_B^+\left[B\right]}} \quad \text{(C-5)}$$
$$=\frac{\left[E\right]_T/\tilde{k}_2^+}{\frac{1}{\tilde{k}_2^+}+\frac{1}{k_A^+\left[A\right]}+\frac{1}{k_B^+\left[B\right]}-\frac{1}{k_A^+\left[A\right]+k_B^+\left[B\right]}}$$

When $\left[EAB\right]$ from equation of (C-5) is entered into equation (9), we then obtain equation (26).

Appendix D: Deriving the SUPECA kinetics equation (28)

We first derive the set of linear equations using the first order closure approach (i.e., the perturbation method truncated to first order accuracy; Shankar, 1994; Tang et al., 2007). By entering equations (14)-(16) into equation (23), we have

$$k_B^+\left[EA\right]\left(\left[B\right]_T-\left[EB\right]-\left[EAB\right]\right)=k_A^+\left(\left[A\right]_T-\left[EA\right]-\left[EAB\right]\right)\\ \times\left(\left[E\right]_T-\left[EA\right]-\left[EB\right]-\left[EAB\right]\right) \tag{D-1}$$

Now if we expand equation (D-1), and keep only the zero and the first order term of $\left[EA\right]$, $\left[EB\right]$ and $\left[EAB\right]$, then we obtain

$$k_B^+\left[B\right]_T\left[EA\right]=k_A^+\left[E\right]_T\left(\left[A\right]_T-\left[EA\right]-\left[EAB\right]\right)\\ -k_A^+\left[A\right]_T\left(\left[EA\right]+\left[EB\right]+\left[EAB\right]\right) \tag{D-2}$$

which after some rearrangement becomes

$$\left(k_A^+\left[A\right]_T+k_A^+\left[E\right]_T+k_B^+\left[B\right]_T\right)\left[EA\right]+k_A^+\left[A\right]_T\left[EB\right]\\ +k_A^+\left(\left[A\right]_T+\left[E\right]_T\right)\left[EAB\right]=k_A^+\left[A\right]_T\left[E\right]_T \tag{D-3}$$

Using the definitions of $f_A=k_A^+\left[A\right]_T$, $f_B=k_B^+\left[B\right]_T$ and $\overline{f}_A=f_A+k_A^+\left[E\right]_T$, we may rewrite equation (D-3) as

$$\left(\overline{f}_A+f_B\right)\left[EA\right]+f_A\left[EB\right]+\overline{f}_A\left[EAB\right]=f_A\left[E\right]_T \tag{D-4}$$

Because substrates A and B are symmetric in forming the consumer substrate complexes, a similar linear equation can be derived by switching A and B in equation (D-4) (or by repeating procedures to the derivation of equation (D-4) but using equations (14)-(16) and (24))

$$f_B\left[EA\right]+\left(f_A+\overline{f}_B\right)\left[EB\right]+\overline{f}_B\left[EAB\right]=f_B\left[E\right]_T \tag{D-5}$$

Now substitute equations (14)-(16), (23) and (24) into equation (25) and assume $\tilde{k}_2^+\approx k_2^+$ (i.e., unbinding is much smaller compared to the product genesis rate), we have

$$\left\{k_A^+\left(\left[A\right]_T-\left[EA\right]-\left[EAB\right]\right)+k_B^+\left(\left[B\right]_T-\left[EB\right]-\left[EAB\right]\right)\right\}$$
$$\times\left(\left[E\right]_T-\left[EA\right]-\left[EB\right]-\left[EAB\right]\right)=k_2^+\left[EAB\right] \tag{D-6}$$

Once again, by dropping the second and higher order terms of the consumer-substrate complexes, equation (D-6) can be reduced to

$$\left(k_A^+\left[A\right]_T+k_B^+\left[B\right]_T\right)\left[E\right]_T=\left(k_A^+\left[A\right]_T+k_B^+\left[B\right]_T\right)$$
$$\times\left(\left[EA\right]+\left[EB\right]+\left[EAB\right]\right)+k_A^+\left[E\right]_T\left(\left[EA\right]+\left[EAB\right]\right) \tag{D-7}$$
$$+k_B^+\left[E\right]_T\left(\left[EB\right]+\left[EAB\right]\right)+k_2^+\left[EAB\right]$$

which by aid of $f_A=k_A^+\left[A\right]_T$, $f_B=k_B^+\left[B\right]_T$, $\overline{f}_A=f_A+k_A^+\left[E\right]_T$, $\overline{f}_B=f_B+k_B^+\left[E\right]_T$,

$f_{AB}=f_A+f_B$, and $\overline{f}_{AB}=\overline{f}_A+\overline{f}_B$ becomes

$$\left(\overline{f}_A+f_B\right)\left[EA\right]+\left(f_A+\overline{f}_B\right)\left[EB\right]+\left(k_2^+ +\overline{f}_{AB}\right)\left[EAB\right]=f_{AB}\left[E\right]_T \tag{D-8}$$

Now we solve for $\left[EAB\right]$ from the set of linear equations (D-4), (D-5) and (D-8) using Cramer's rule (e.g., Habgood and Arel, 2012), and find the denominator as

$$\det\left(M_d\right)=\begin{vmatrix}\overline{f}_A+f_B & f_A & \overline{f}_A\\ f_B & f_A+\overline{f}_B & \overline{f}_B\\ \overline{f}_A+f_B & f_A+\overline{f}_B & k_2^+ +\overline{f}_{AB}\end{vmatrix} \tag{D-9}$$

and the numerator as

$$\det\left(M_n\right)=\left[E\right]_T\begin{vmatrix}\overline{f}_A+f_B & f_A & f_A\\ f_B & f_A+\overline{f}_B & f_B\\ \overline{f}_A+f_B & f_A+\overline{f}_B & f_{AB}\end{vmatrix} \tag{D-10}$$

Equations (D-9) and (D-10) together lead to

$$
\begin{aligned}
\left[EAB\right] &= \frac{\det\left(M_n\right)}{\det\left(M_d\right)} = \frac{f_A f_B \overline{f}_{AB} \left[E\right]_T}{k_2^+\left(f_A\overline{f}_A + f_B\overline{f}_B + \overline{f}_A\overline{f}_B\right) + \overline{f}_A\overline{f}_B f_{AB}} \\
&= \frac{f_A f_B \overline{f}_{AB} \left[E\right]_T}{k_2^+\left(f_{AB}\overline{f}_{AB} - f_A\overline{f}_B - \overline{f}_A f_B + \overline{f}_A\overline{f}_B\right) + \overline{f}_A\overline{f}_B f_{AB}} \\
&= \frac{\left[E\right]_T}{k_2^+\left(\frac{f_{AB}}{f_A f_B} - \frac{f_A\overline{f}_B + \overline{f}_A f_B - \overline{f}_A\overline{f}_B}{f_A f_B \overline{f}_{AB}}\right) + \frac{\overline{f}_A\overline{f}_B f_{AB}}{f_A f_B \overline{f}_{AB}}} \\
&= \frac{\left[E\right]_T \Big/ k_2^+}{\frac{1}{k_2^+}\frac{\overline{f}_A\overline{f}_B f_{AB}}{f_A f_B \overline{f}_{AB}} + \left(\frac{1}{f_A} + \frac{1}{f_B} - \frac{f_A\overline{f}_B + \overline{f}_A f_B - \overline{f}_A\overline{f}_B}{f_A f_B \overline{f}_{AB}}\right)}
\end{aligned}
\tag{D-11}
$$

which, when entered into equation (9), leads to equation (28).

Appendix E: Deriving SUPECA for a network of substrates and consumers

In the second equation of equation (33), we show that the consumption of a certain substrate as represented in ECA kinetics is determined by the consumer reaction potential $k_{2,ij}^+\left[E_j\right]_T$ multiplied with the relative contribution of the specific consumption pathway with respect to all competing pathways ($F_{c,j}^{\{r\}} \Big/ \left(1 + F_{r,j} + F_{c,j}\right)$). Since SUPECA kinetics is a compatible extension of the ECA kinetics, SUPECA kinetics should have its numerator indicating the potential reaction rate of the specific pathway, and its denominator indicating the efforts of all interacting pathways. Bearing this partition equivalence in mind, therefore, we assert that $\overline{f}_A \big/ k_2^+$ in equation (29) should be equivalent to $F_{r,i} + F_{c,j}$ in equation (33). This assertion then leads to equations (38), (41) and (43) for A substrates. Similarly, equations (39), (42) and (44) are for B substrates. With the definitions of $f_A \big/ k_2^+$, $f_B \big/ k_2^+$, $\overline{f}_A \big/ k_2^+$ and $\overline{f}_B \big/ k_2^+$, using the partition

equivalence, we can easily define the network form of f_{AB} in equation (40), and the network form of $\overline{f}_{AB}$ in equation (45). Further, we observe that the denominator of the last equation in equation (28) could be rewritten as

$$\frac{\left(\overline{f}_A/k_2^+\right)\left(\overline{f}_B/k_2^+\right)\left(f_{AB}/k_2^+\right)}{\left(\overline{f}_{AB}/k_2^+\right)}+\left(f_{AB}/k_2^+\right)-\frac{\left(f_A/k_2^+\right)\left(\overline{f}_B/k_2^+\right)+\left(\overline{f}_A/k_2^+\right)\left(f_B/k_2^+\right)-\left(\overline{f}_A/k_2^+\right)\left(\overline{f}_B/k_2^+\right)}{\left(\overline{f}_{AB}/k_2^+\right)}$$

which, after replacing f_A/k_2^+, f_B/k_2^+, $\overline{f}_A/k_2^+$, $\overline{f}_B/k_2^+$, f_{AB}/k_2^+ and $\overline{f}_{AB}/k_2^+$ with their corresponding network forms (i.e. equations (38)-(45)), leads to SUPECA kinetics equation (37).

Appendix F: Formulation of the kinetics-benchmarking problem

Following equations (23)-(25), the Equilibrium Chemistry (EC) problem used to benchmark synthesizing unit (SU) and SUPECA predictions is defined as

$$k_{BS1}\left[B\right]\left[S_1\right]=k_{BS2}\left[S_2\right]\left[BS_1\right] \tag{F-1}$$

$$k_{BS2}\left[B\right]\left[S_2\right]=k_{BS1}\left[S_1\right]\left[BS_2\right] \tag{F-2}$$

$$k_{BS1}\left[BS_2\right]\left[S_1\right]+k_{BS2}\left[BS_1\right]\left[S_2\right]=k_2^+\left[BS_1S_2\right] \tag{F-3}$$

$$K_{MS1}\left[MS_1\right]=\left[M\right]\left[S_1\right] \tag{F-4}$$

which are subject to the constraints

$$\left[S_1\right]_T=\left[S_1\right]+\left[MS_1\right]+\left[BS_1\right]+\left[BS_1S_2\right] \tag{F-5}$$

$$\left[S_2\right]_T=\left[S_2\right]+\left[BS_2\right]+\left[BS_1S_2\right] \tag{F-6}$$

$$\left[B\right]_T=\left[B\right]+\left[BS_1\right]+\left[BS_2\right]+\left[BS_1S_2\right] \tag{F-7}$$

$$\left[M\right]_T = \left[M\right] + \left[MS_1\right] \quad \text{(F-8)}$$

To relate these equations to a dynamic system, S_1 and S_2 are substrates, B is microbial population, and M is some sorbent that can reversibly adsorb substrate S_1.

For benchmarking, $\left[BS_1S_2\right]$ is solved from equations (F-1)-(F-8) using a fixed-point iteration algorithm (see supplemental materials) for each set of parameters. Unlike the Newton-Raphson iteration, the fixed-point iteration ensures positive mass of all variables, and mass balance relationships from (F-5)-(F-8) are automatically satisfied by the numerical solution.

Appendix G: Derivation of relevant kinetic parameters for the steady state aerobic respiration problem

The aerobic respiration problem is formulated as

$$\frac{d\left[\mathrm{O}_2\right]_{g,s}}{dt} = \frac{\left(\left[\mathrm{O}_2\right]_a - \left[\mathrm{O}_2\right]_{g,s}\right)}{\left(R_a + R_s\right)Z} - F\left(B, \left[\mathrm{O}_2\right]_{g,s}, S, M\right) \quad \text{(G-1)}$$

where $\left[O_2\right]_{g,s}$ is gaseous oxygen concentration in bulk soil. $\left[O_2\right]_a$ is atmospheric oxygen concentration (set to 8.45 mol m^{-3}). S is dissolvable organic carbon concentration (set to 3 mol m^{-3}), and M is soil mineral sorbent concentration (with variable values). All concentrations are defined with unit mol m^{-3}. R_a is aerodynamic resistance, which is set to 50 s m^{-1}. R_s is soil resistance (s m^{-1}) calculated using the approach in Tang and Riley (2013b). Z is soil depth (set to 10 cm). $F\left(B, \left[O_2\right]_{g,s}, S, M\right)$ is the oxygen consumption rate calculated using the SUPECA kinetics, whose kinetic parameters are derived as

following. The steady-state problem is solved by setting the temporal derivative of equation (G-1) to zero, and solved for $\left[O_2\right]_{g,s}$ through iterations. The shape of the flux $F\left(B,\left[O_2\right]_{g,s},S,M\right)$ is then compared to that derived from incubation studies in Franzluebbers (1999).

In this aerobic respiration problem, microbes are assumed to form microsites sitting uniformly inside pores of the bulk soil. O_2 approaches the microsites through both aqueous and gaseous diffusion, and only aqueous phase is used for microbial respiration. This leads to the relationship between near cell aqueous O_2 concentration and the diffusive flux as

$$v_m \frac{d\left[\mathrm{O}_2\right]_{w,0}}{dt} = -k_{02,w,1}\left[X\right]\left[\mathrm{O}_2\right]_{w,0} + \kappa_{02}\left(\left[\mathrm{O}_2\right]_w - \left[\mathrm{O}_2\right]_0\right) \tag{G-2}$$

where the conductance κ_{02} is

$$\left(\frac{\kappa_{02}}{4\pi}\right)^{-1} = \frac{\delta}{D_{w,02} r_m \left(r_m + \delta\right)} + \frac{1}{D_{02}\left(r_m + \delta\right)} \tag{G-3}$$

where r_m is the radius of the microsite (or aggregate), δ is thickness of the water film that covers the microsite (Grant and Rochette, 1994), v_m is the microsite volume (m^3 $site^{-1}$), and $\left[\mathrm{O}_2\right]$ is the aqueous oxygen concentration in the bulk soil matrix. $\left[X\right]$ is the cell density (mol cell $site^{-1}$). The unit of $k_{02,1}$ is then m^3 (mol cell)$^{-1}$ s^{-1}.

The bulk aqueous diffusivity in equation (G-3) is

$$D_{02} = \theta D_{02,w} + \frac{\varepsilon}{\alpha_{02}} D_{02,g} \tag{G-4}$$

Now if we assume steady state (aka $d\left[O_2\right]_0 \big/ dt \approx 0$) of equation (G-2), we then obtain

$$\left[\mathrm{O}_2\right]_{w,0} = \frac{\left[\mathrm{O}_2\right]_w}{1+\dfrac{k_{\mathrm{O2},w,1}\left[X\right]}{\kappa_{O2}}} \tag{G-5}$$

which leads to the revised the affinity parameter as

$$\tilde{K}_{\mathrm{O2}} = \frac{k_2}{k_{\mathrm{O2},w,1}}\left(1+\frac{k_{\mathrm{O2},w,1}\left[X\right]_T}{\kappa_{O2}}\right) \tag{G-6}$$

where the zero order approximation is made by taking $\left[X\right] \approx \left[X\right]_T$.

Now assume that the ball-like microbe is covered with N disc-like porters, whose mean radius is r_p. Assuming that the binding is limited by diffusion, then using the chemoreception theory by Berg and Purcell (1977), we have

$$k_{\mathrm{O2},w,1} = 4\pi D_{\mathrm{O2},w,0} r_c \frac{Nr_p}{Nr_p+\pi r_c}\,\mathrm{cell}^{-1} \tag{G-7}$$

where the term $Nr_p \big/ \left(Nr_p+\pi r_c\right)$ accounts for the interference between different porters of a cell. Thus assuming $\left[X\right]_T = m$ cell site^{-1}, we get

$$\tilde{K}_{\mathrm{O2}} = \frac{k_2}{k_{\mathrm{O2},w,1}}\left(1+\frac{k_{\mathrm{O2},1}\left[X\right]_T}{\kappa_{\mathrm{O2}}}\right) = K_{\mathrm{O2,w}}\left(1+\frac{Nr_p}{Nr_p+\pi r_c}\frac{mr_c}{r_m+\delta}\left(\frac{\delta}{r_m}+\frac{D_{\mathrm{O2},w,0}}{D_{O2}}\right)\right) \tag{G-8}$$

With similar procedure, for DOC we have the following

$$\tilde{K}_{\mathrm{DOC}} = \frac{k_2}{k_{\mathrm{DOC},w,1}}\left(1+\frac{k_{\mathrm{DOC},w,1}\left[X\right]_T}{\kappa_{DOC}}\right) = K_{\mathrm{DOC}}\left(1+\frac{Nr_p}{Nr_p+\pi r_c}\frac{mr_c}{r_m+\delta}\left(\frac{\delta}{r_m}+\frac{D_{DOC,w,0}}{D_{DOC}}\right)\right) \tag{G-9}$$

and

$$k_{\mathrm{DOC},w,1} = 4\pi D_{\mathrm{DOC},w,0} r_c N_A \frac{N r_p}{N r_p + \pi r_c} \left(\mathrm{mol}\cdot\mathrm{cell}\right)^{-1} \quad \text{(G-10)}$$

where $N_A = 6.02\times10^{23}\,\mathrm{mol}^{-1}$.

Below we provide some estimates for the parameters to support the above model of moisture dependence of microbial decomposition. The microbial cell radius r_c is on the order of 10^{-6} m, and r_p/r_c is about 10^{-3}. At 25 °C, the aqueous diffusivity of O_2 is about 2.9×10^{-9} m^2 s^{-1}, therefore, assuming $N = 3000$ porters per cell (which covers only 0.3% of the cell's surface area), we have $k_{\mathrm{O2},w,1} = 1.0\times10^{10}$ m^3 $\left(\mathrm{mol\ cell}\right)^{-1}\mathrm{s}^{-1}$. Similarly, since the aqueous diffusivity of DOC is about 10^{-9} m^2 s^{-1}, assuming $N = 3000$ porters per cell, we have $k_{\mathrm{DOC},w,1} = 3.7\times10^{9}$ m^3 $\left(\mathrm{mol\ cell}\right)^{-1}\mathrm{s}^{-1}$. Suppose the respiration is bottlenecked by a single respiratory enzyme, and since the enzyme activity varies on the order of 10~1000 s^{-1} (English et al., 2006), then by taking $k_2 = 100N$ $\mathrm{s}^{-1} = 3\times10^{5}\mathrm{s}^{-1}$ per cell, we have $K_{\mathrm{O2,w}} = 3\times10^{-5}$ mol m^{-3}, which agrees well with parameters reported for microbes in aqueous solutions in Button (1985). However, Grant (1991) estimated $K_{\mathrm{O2,w}} = 3.0\times10^{-3}$ mol m^{-3}; Borden and Bedient (1986) estimated $K_{\mathrm{O2,w}} = 3.1\times10^{-3}$ mol m^{-3} for application in soil. We therefore elevated the numerical value to $K_{\mathrm{O2,w}} = 3.0\times10^{-3}$ mol m^{-3}. According to equations (G-7) and (G-8), such elevation could occur either by increasing the maximum substrate processing rate k_2 or

decreasing the diffusion $k_{O2,w,1}$ controlled parameter (through the formation of micro-pores in aggregates; e.g., Kausch and Pallud, 2013; Yang et al., 2014). Based on similar magnitude analysis, we obtain $K_{DOC,w} = 8.1\times10^{-5}\,\mathrm{mol\,m^{-3}}$, which falls to the lower end of the values reported for many hydrocarbon compounds as reported in Button (1985). We did not elevate the value of $K_{DOC,w}$ because it could vary over four orders of magnitudes (Button, 1985), and our number leads to a good fit between model predictions and data.

Taking all these numbers together, we have

$$\begin{aligned}\tilde{K}_{O2,w} &= K_{O2,w}\left(1+0.48\times\frac{mr_c}{r_m+\delta}\left(\frac{\delta}{r_m}+\frac{D_{O2,w,0}}{D_{O2}}\right)\right)\\ &= 3\times10^{-3}\left(1+0.48\times\frac{mr_c}{r_m+\delta}\left(\frac{\delta}{r_m}+\frac{D_{O2,w,0}}{D_{O2}}\right)\right)\end{aligned} \tag{G-11}$$

$$\begin{aligned}\tilde{K}_{DOC} &= K_{DOC}\left(1+0.48\times\frac{mr_c}{r_m+\delta}\left(\frac{\delta}{r_m}+\frac{D_{DOC,w,0}}{D_{DOC}}\right)\right)\\ &= 8.1\times10^{-5}\left(1+0.48\times\frac{mr_c}{r_m+\delta}\left(\frac{\delta}{r_m}+\frac{D_{DOC,w,0}}{D_{DOC}}\right)\right)\end{aligned} \tag{G-12}$$

Since at 25 °C, the Bunsen solubility coefficient of oxygen is 0.032, we have

$$\tilde{K}_{O2,g} = \frac{\tilde{K}_{O2,w}}{0.032} = 9.4\times10^{-2}\left(1+0.48\times\frac{mr_c}{r_m+\delta}\left(\frac{\delta}{r_m}+\frac{D_{O2,w,0}}{D_{O2}}\right)\right) \tag{G-13}$$

The water film thickness is a function of soil water potential (Tokunaga, 2009) and we calculate it using the approach in ECOSYS (Grant, 2001), which is

$$\delta = \max\left(10^{-6}, \exp\left(-13.65-0.857\log\left(-\psi\right)\right)\right) \tag{G-14}$$

where the soil matric potential is of unit m, and water film thickness is restricted to at least 1 μm.

For model applications, the microbes are often in the unit of mol C m^{-3}. Bratbak and Dundas (1984) reported that the wet biomass density of bacteria is over the range 1.1~1.2 g cm^{-3}, of which about 40% is dry biomass, and about 50% of dry biomass is carbon. Therefore, with the medium cell density 1.15 g cm^{-3}, 1 mol C m^{-3} microbial biomass is about 52.17 cm^3, by further taking $r_c = 10^{-6}$ m=10^{-4} cm, the cell number density is 2.1×10^{-11} mol cell m^{-3}. Therefore, for $k_2 = 100\ s^{-1}$ per porter, given each cell has 3000 porters, the maximum respiration rate is 6.3×10^{-6} s^{-1} for 1 mol C m^{-3} dry microbial biomass, which was then elevated to 3.8×10^{-4} s^{-1} to obtain a better fitting between data and model prediction. This required elevation in maximum respiration rate indicates that the data as obtained (after 24 days of incubation) in Franzluebbers (1999) are representative of fast growing microbes.

Author Contributions

J.Y. Tang designed the theory and conducted the analysis. J.Y. Tang and W.J. Riley discussed the results and wrote the paper.

Acknowledgements

This research was supported by the Director, Office of Science, Office of Biological and Environmental Research of the US Department of Energy under contract No. DE-AC02-05CH11231 as part of the Accelerated Climate Model for Energy in the Earth system Modeling program and the Next Generation Ecosystem Experiment-Arctic project.

Financial support does not constitute an endorsement by the Department of Energy of the views expressed in this study.

References

Aksnes, D. L. and Egge, J. K.: A theoretical-model for nutrient-uptake in phytoplankton, Mar Ecol Prog Ser, 70, 65-72, 1991.

Allison, S. D.: A trait-based approach for modelling microbial litter decomposition, Ecol Lett, 15, 1058-1070, 2012.

Armstrong, R. A.: Nutrient uptake rate as a function of cell size and surface transporter density: A Michaelis-like approximation to the model of Pasciak and Gavis, Deep-Sea Res Pt I, 55, 1311-1317, 2008.

Arora, V. K., Boer, G. J., Friedlingstein, P., Eby, M., Jones, C. D., Christian, J. R., Bonan, G., Bopp, L., Brovkin, V., Cadule, P., Hajima, T., Ilyina, T., Lindsay, K., Tjiputra, J. F., and Wu, T.: Carbon-Concentration and Carbon-Climate Feedbacks in CMIP5 Earth System Models, J Climate, 26, 5289-5314, 2013.

Batjes, N. H.: Harmonized soil property values for broad-scale modelling (WISE30sec) with estimates of global soil carbon stocks, Geoderma, 269, 61-68, 2016.

Berg, H. C. and Purcell, E. M.: Physics of Chemoreception, Biophys J, 20, 193-219, 1977.

Blanke, J. H., Lindeskog, M., Lindstrom, J., and Lehsten, V.: Effect of climate data on simulated carbon and nitrogen balances for Europe, J Geophys Res-Biogeo, 121, 1352-1371, 2016.

Bonachela, J. A., Raghib, M., and Levin, S. A.: Dynamic model of flexible phytoplankton nutrient uptake, P Natl Acad Sci USA, 108, 20633-20638, 2011.

Borden, R. C. and Bedient, P. B.: Transport of dissolved hydrocarbons influenced by oxygen-limited biodegradation .1. Theoretical development, Water Resour Res, 22, 1973-1982, 1986.

Borghans, J. A. M., DeBoer, R. J., and Segel, L. A.: Extending the quasi-steady state approximation by changing variables, B Math Biol, 58, 43-63, 1996.

Bouskill, N. J., Tang, J.Y., Riley, W. J., and Brodie, E. L.: Trait-based representation of biological nitr fication: model development testing, and predicted community

composition, Front Microbiol, 3, 2012.
Bouskill, N. J., Riley, W. J., and Tang, J. Y.: Meta-analysis of high-latitude nitrogen-addition and warming studies implies ecological mechanisms overlooked by land models, Biogeosciences, 11, 6969-6983, 2014.
Brandt, B. W., van Leeuwen, I. M. M., and Kooijman, S. A. L. M.: A general model for multiple substrate biodegradation. Application to co-metabolism of structurally non-analogous compounds, Water Res, 37, 4843-4854, 2003.
Bratbak, G. and Dundas, I.: Bacterial dry-matter content and biomass estimations, Appl Environ Microb, 48, 755-757, 1984.
Briggs, G. E. and Haldane, J. B. S.: A note on the kinetics of enzyme action, Biochem J, 19, 338-339, 1925.
Button, D. K.: Kinetics of nutrient-limited transport and microbial-growth, Microbiol Rev, 49, 270-297, 1985.
Chellaboina, V., Bhat, S. P., Haddad, W. M., and Bernstein, D. S.: Modeling and analysis of mass-action kinetics, nonnegativity, realizability, reducibility, and semistability, IEEE Contr Syst Mag, 29, 60-78, 2009.
Ciais, P., Gasser, T., Paris, J. D., Caldeira, K., Raupach, M. R., Canadell, J. G., Patwardhan, A., Friedlingstein, P., Piao, S. L., and Gitz, V.: Attributing the increase in atmospheric CO_2 to emitters and absorbers, Nat Clim Change, 3, 926-930, 2013.
English, B. P., Min, W., van Oijen, A. M., Lee, K. T., Luo, G. B., Sun, H. Y., Cherayil, B. J., Kou, S. C., and Xie, S. N.: Ever-fluctuating single enzyme molecules: Michaelis-Menten equation revisited (vol 2, pg 87, 2006), Nat Chem Biol, 2, 168-168, 2006.
Franzluebbers, A. J.: Microbial activity in response to water-filled pore space of variably eroded southern Piedmont soils, Appl Soil Ecol, 11, 91-101, 1999.
Feyman, R.P., Leighton, R.B., and Sands, M.: The Feynman lectures on physics: Vol. I., Addison-Wesley Publishing Company, Inc., Reading, Massachusetts, 1963
Friedlingstein, P., Meinshausen, M., Arora, V. K., Jones, C. D., Anav, A., Liddicoat, S. K., and Knutti, R.: Uncertainties in CMIP5 Climate Projections due to carbon cycle feedbacks, J Climate, 27, 511-526, 2014.
Grant, R. F.: A Technique for estimating denitrification rates at different soil temperatures, water Contents, and nitrate concentrations, Soil Sci, 152, 41-52, 1991.

Grant, R. F. and Rochette, P.: Soil microbial respiration at different water potentials and temperatures - theory and mathematical-modeling, Soil Sci Soc Am J, 58, 1681-1690, 1994.
Grant, R.F.: A review of the canadian ecosystem Model-Ecosys, in Modeling carbon and nitrogen dynamics for soil management, 173-264, 2001.
Griffin, D. M.: A Theoretical study relating concentration and diffusion of oxygen to biology of organisms in soil, New Phytol, 67, 561-577, 1968.
Gross, D., Shortle, J.F., Thompson, J.M. and Harris, C.M.: Fundamentals of queueing theory, ISBN: 978-1-118-21164-9, Wiley series in probability and statistics, 2011.
He, Y. J., Trumbore, S. E., Torn, M. S., Harden, J. W., Vaughn, L. J. S., Allison, S. D., and Randerson, J. T.: Radiocarbon constraints imply reduced carbon uptake by soils during the 21st century, Science, 353, 1419-1424, 2016.
Holling, C. S.: Some characteristics of simple types of predation and parasitism, Can. Entomol., 91, 385–398, doi:10.4039/Ent91385-7, 1959.
Holling, C.S.: The functional response of invertebrate predators to prey density, Mem. Entomol. Soc. Can., 48, 1-86, 1966.
Iwasa, Y., Andreasen, V., and Levin, S.: Aggregation in Model-Ecosystems .1. Perfect Aggregation, Ecol Model, 37, 287-302, 1987.
Iwasa, Y., Levin, S. A., and Andreasen, V.: Aggregation in Model-Ecosystems .2. Approximate Aggregation, Ima J Math Appl Med, 6, 1-23, 1989.
Kausch, M. F. and Pallud, C. E.: Modeling the impact of soil aggregate size on selenium immobilization, Biogeosciences, 10, 1323-1336, 2013.
Kolditz, O., Ratke, R., Diersch, H. J. G., and Zielke, W.: Coupled groundwater flow and transport .1. Verification of variable density flow and transport models, Adv Water Resour, 21, 27-46, 1998.
Kooijman, S. A. L. M.: The Synthesizing Unit as model for the stoichiometric fusion and branching of metabolic fluxes, Biophys Chem, 73, 179-188, 1998.
Kooijman, S.: Dynamic energy budget theory for metabolic organisation. Cambridge University Press, Cambridge, 2010.
Koven, C. D., Riley, W. J., Subin, Z. M., Tang, J. Y., Torn, M. S., Collins, W. D., Bonan, G. B., Lawrence, D. M., and Swenson, S. C.: The effect of vertically resolved soil

biogeochemistry and alternate soil C and N models on C dynamics of CLM4, Biogeosciences, 10, 7109-7131, 2013.
Le Roux, X., Bouskill, N. J., Niboyet, A., Barthes, L., Dijkstra, P., Field, C. B., Hungate, B. A., Lerondelle, C., Pommier, T., Tang, J. Y., Terada, A., Tourna, M., and Poly, F.: Predicting the responses of soil nitrite-oxidizers to multi-factorial global change: A trait-based approach, Front Microbiol, 7, 2016.
Litchman, E. and Klausmeier, C. A.: Trait-based community ecology of phytoplankton, Annu Rev Ecol Evol S, 39, 615-639, 2008.
Luo, Z., Wang, E., Zheng, H., Baldock, J. A., Sun, O. J., and Shao, Q.: Convergent modelling of past soil organic carbon stocks but divergent projections, Biogeosciences, 12, 4373-4383, 2015.
Manzoni, S., Moyano, F., Katterer, T., and Schimel, J.: Modeling coupled enzymatic and solute transport controls on decomposition in drying soils, Soil Biol Biochem, 95, 275-287, 2016.
Mao, X., Prommer, H., Barry, D. A., Langevin, C. D., Panteleit, B., and Li, L.: Three-dimensional model for multi-component reactive transport with variable density groundwater flow, Environ Modell Softw, 21, 615-628, 2006.
Michaelis, L. and Menten, M. L.: The kenetics of the inversion effect, Biochem. Z., 49, 333–369, 1913.
Monod, J.: The growth of bacterial cultures, Annu Rev Microbiol, 3, 371-394, 1949.
Murdoch, W. W.: Functional response of predators, J Appl Ecol, 10, 335-342, 1973.
Oleson, K.W. et al.: Technical description of version 4.5 of the Community Land Model (CLM). Ncar TechRep., Note NCAR/TN-503+ STR. National Center for Atmospheric Research, Boulder, CO, 422 pp. doi: 10.5065/D6RR1W7M, 2013
Pedersen, M. G., Bersani, A. M., and Bersani, E.: Quasi steady-state approximations in complex intracellular signal transduction networks - a word of caution, J Math Chem, 43, 1318-1344, 2008.
Pyun, C. W.: Steady-state and equilibrium approximations in chemical kinetics, J Chem Educ, 48, 194-&, 1971.
Qian, Y., Yan, H. P., Hou, Z. S., Johannesson, G., Klein, S., Lucas, D., Neale, R., Rasch, P., Swiler, L., Tannahill, J., Wang, H. L., Wang, M. H., and Zhao, C.: Parametric

sensitivity analysis of precipitation at global and local scales in the Community Atmosphere Model CAM5, J Adv Model Earth Sy, 7, 382-411, 2015.
Renault, P. and Stengel, P.: Modeling oxygen diffusion in aggregated Soils .1. Anaerobiosis inside the aggregates, Soil Sci Soc Am J, 58, 1017-1023, 1994.
Resat, H., Bailey, V., McCue, L.A., and Konopka, A.: Modeling microbial dynamics in heterogeneous environments: growth on soil carbon sources, Microb. Ecol., doi:10.1007/s00248-011-9965-x, 2011.
Reuveni, S., Urbakh, M., and Klafter, J.: Role of substrate unbinding in Michaelis-Menten enzymatic reactions, P Natl Acad Sci USA, 111, 4391-4396, 2014.
Riley, W. J., Subin, Z. M., Lawrence, D. M., Swenson, S. C., Torn, M. S., Meng, L., Mahowald, N. M., and Hess, P.: Barriers to predicting changes in global terrestrial methane fluxes: analyses using CLM4Me, a methane biogeochemistry model integrated in CESM, Biogeosciences, 8, 1925-1953, 2011.
Riley, W. J., Maggi, F., Kleber, M., Torn, M. S., Tang, J. Y., Dwivedi, D., and Guerry, N.: Long residence times of rapidly decomposable soil organic matter: application of a multi-phase, multi-component, and vertically resolved model (BAMS1) to soil carbon dynamics, Geosci Model Dev, 7, 1335-1355, 2014.
Schnell, S. and Maini, P. K.: Enzyme kinetics at high enzyme concentration, B Math Biol, 62, 483-499, 2000.
Schnell, S. and Mendoza, C.: Enzyme kinetics of multiple alternative substrates, J Math Chem, 27, 155-170, 2000.
Shankar, R.: Principles of quantum mechanics, second edition, Springer, ISBN 978-1-4757-0578-2, 1994.
Shao, P., Zeng, X. B., Sakaguchi, K., Monson, R. K., and Zeng, X. D.: Terrestrial carbon cycle: climate relations in eight CMIP5 earth system models, J Climate, 26, 8744-8764, 2013.
Shi, M., Fisher, J. B., Brzostek, E. R., and Phillips, R. P.: Carbon cost of plant nitrogen acquisition: global carbon cycle impact from an improved plant nitrogen cycle in the Community Land Model, Global Change Biol, 22, 1299-1314, 2016.
Sulman, B. N., Phillips, R. P., Oishi, A. C., Shevliakova, E., and Pacala, S. W.: Microbe-driven turnover offsets mineral-mediated storage of soil carbon under elevated CO2, Nat

Clim Change, 4, 1099-1102, 2014.
Tang, J. Y., Tang, J., and Wang, Y.: Analytical investigation on 3D non-Boussinesq mountain wave drag for wind profiles with vertical variations, Appl Math Mech-Engl, 28, 317-325, 2007.
Tang, J. Y. and Zhuang, Q. L.: Equifinality in parameterization of process-based biogeochemistry models: A significant uncertainty source to the estimation of regional carbon dynamics, J Geophys Res-Biogeo, 113, 2008.
Tang, J. Y. and Zhuang, Q. L.: A global sensitivity analysis and Bayesian inference framework for improving the parameter estimation and prediction of a process-based Terrestrial Ecosystem Model, J Geophys Res-Atmos, 114, 2009.
Tang, J.Y., Zhuang, Q., Shannon, R. D., and White, J. R.: Quantifying wetland methane emissions with process-based models of different complexities, Biogeosciences, 7, 3817-3837, 2010.
Tang, J. Y. and Riley, W. J.: A total quasi-steady-state formulation of substrate uptake kinetics in complex networks and an example application to microbial litter decomposition, Biogeosciences, 10, 8329-8351, 2013a.
Tang, J. Y. and Riley, W. J.: A new top boundary condition for modeling surface diffusive exchange of a generic volatile tracer: theoretical analysis and application to soil evaporation, Hydrol Earth Syst Sc, 17, 873-893, 2013b.
Tang, J. Y., Riley, W. J., Koven, C. D., and Subin, Z. M.: CLM4-BeTR, a generic biogeochemical transport and reaction module for CLM4: model development, evaluation, and application, Geosci Model Dev, 6, 127-140, 2013.
Tang, J. Y. and Riley, W. J.: Weaker soil carbon-climate feedbacks resulting from microbial and abiotic interactions, Nat Clim Change, 5, 56-60, 2015.
Tang, J. Y.: On the relationships between the Michaelis-Menten kinetics, reverse Michaelis-Menten kinetics, equilibrium chemistry approximation kinetics, and quadratic kinetics, Geosci Model Dev, 8, 3823-3835, 2015.
Tang, J. Y. and Riley, W. J.: Technical Note: A generic law-of-the-minimum flux limiter for simulating substrate limitation in biogeochemical models, Biogeosciences, 13, 723-735, 2016.
Tilman, D.: Resource competition and community structure, Princeton University Press,

Princeton, New Jersey, 1982.
Todd-Brown, K. E. O., Randerson, J. T., Post, W. M., Hoffman, F. M., Tarnocai, C., Schuur, E. A. G., and Allison, S. D.: Causes of variation in soil carbon simulations from CMIP5 Earth system models and comparison with observations, Biogeosciences, 10, 1717-1736, 2013.
Tokunaga, T. K.: Hydraulic properties of adsorbed water films in unsaturated porous media, Water Resour Res, 45, 2009.
Van Slyke, D. D. and Cullen, G. E.: The mode of action of urease and of enzymes in general, J Biol Chem, 19, 141-180, 1914.
van Werkhoven, K., Wagener, T., Reed, P., and Tang, Y.: Sensitivity-guided reduction of parametric dimensionality for multi-objective calibration of watershed models, Adv Water Resour, 32, 1154-1169, 2009.
Vitousek, P.: Nutrient cycling and nutrient use efficiency, Am Nat, 119, 553-572, 1982.
Wang, Y. P., Leuning, R., Cleugh, H. A., and Coppin, P. A.: Parameter estimation in surface exchange models using nonlinear inversion: how many parameters can we estimate and which measurements are most useful?, Global Change Biol, 7, 495-510, 2001.
Wieder, W. R., Bonan, G. B., and Allison, S. D.: Global soil carbon projections are improved by modelling microbial processes, Nat Clim Change, 3, 909-912, 2013.
Wieder, W. R., Grandy, A. S., Kallenbach, C. M., and Bonan, G. B.: Integrating microbial physiology and physio-chemical principles in soils with the MIcrobial-MIneral Carbon Stabilization (MIMICS) model, Biogeosciences, 11, 3899-3917, 2014.
Wieder, W. R., Cleveland, C. C., Lawrence, D. M., and Bonan, G. B.: Effects of model structural uncertainty on carbon cycle projections: biological nitrogen fixation as a case study, Environ Res Lett, 10, 2015a.
Wieder, W. R., Allison, S. D., Davidson, E. A., Georgiou, K., Hararuk, O., He, Y. J., Hopkins, F., Luo, Y. Q., Smith, M. J., Sulman, B., Todd-Brown, K., Wang, Y. P., Xia, J. Y., and Xu, X. F.: Explicitly representing soil microbial processes in Earth system models, Global Biogeochem Cy, 29, 1782-1800, 2015b.
Wieder, W. R., Cleveland, C. C., Smith, W. K., and Todd-Brown, K.: Future productivity and carbon storage limited by terrestrial nutrient availability, Nat Geosci, 8, 441-444,

2015c.
Williams, P. J.: Validity of application of simple kinetic analysis to heterogeneous microbial populations, Limnol Oceanogr, 18, 159-164, 1973.
Williams, M., Schwarz, P. A., Law, B. E., Irvine, J., and Kurpius, M. R.: An improved analysis of forest carbon dynamics using data assimilation, Global Change Biol, 11, 89-105, 2005.
Yang, X. F., Richmond, M. C., Scheibe, T. D., Perkins, W. A., and Resat, H.: Flow partitioning in fully saturated soil aggregates, Transport Porous Med, 103, 295-314, 2014.
Yeh, G. T., Burgos, W. D., and Zachara, J. M.: Modeling and measuring biogeochemical reactions: system consistency, data needs, and rate formulations, Adv Environ Res, 5, 219-237, 2001.
Zhu, Q. and Riley, W. J.: Improved modelling of soil nitrogen losses, Nat Clim Change, 5, 705-706, 2015.
Zhu, Q., Riley, W. J., Tang, J.Y., and Koven, C. D.: Multiple soil nutrient competition between plants, microbes, and mineral surfaces: model development, parameterization, and example applications in several tropical forests, Biogeosciences, 13, 341-363, 2016a.
Zhu, Q., Iversen, C. M., Riley, W. J., Slette, I. J., and Vander Stel, H. M.: Root traits explain observed tundra vegetation nitrogen uptake patterns: Implications for trait-based land models, J. Geophys. Res. Biogeosci., 121, 3101–3112, doi:10.1002/2016JG003554, 2016b.
Zhu, Q., Riley, W. J., and Tang, J. Y.: A new theory of plant-microbe nutrient competition resolves inconsistencies between observations and model predictions, Ecol Appl, 27, 875-886, 2017.

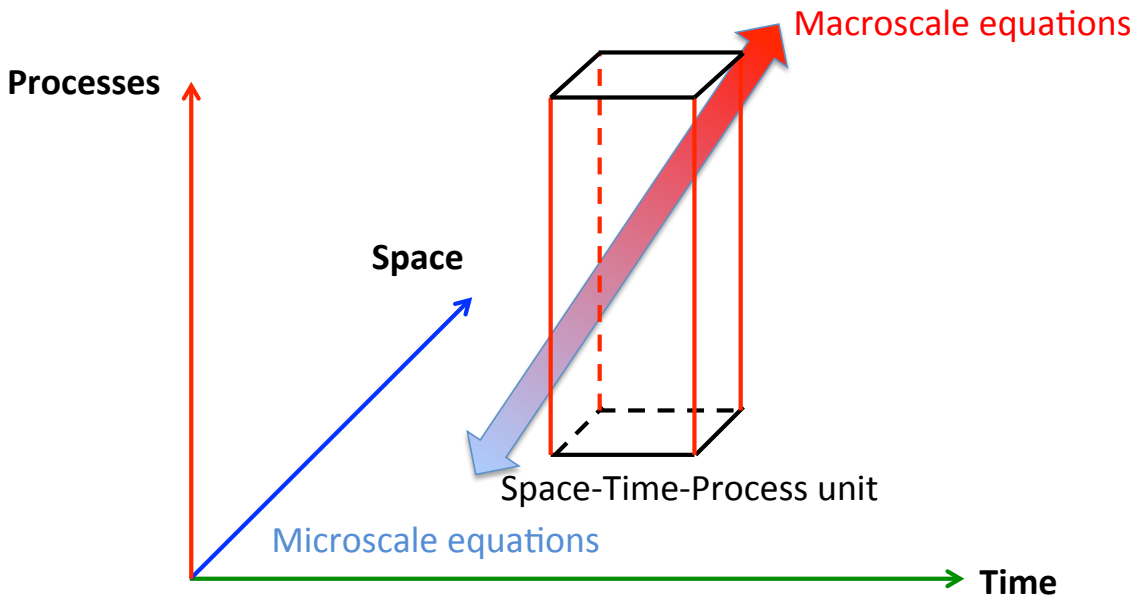

Figure 1. Relationships of the three dimensions involved in the scaling exercise for numerical modeling of biogeochemical systems. In general, as one scales the Space-Time-Process unit from small scales into large scales, the resultant macroscale equations may appear simpler than the microscale equations.

$$F_{c,j} = \sum_{l=1}^{l=I} \left[S_l\right] / K_{lj}$$

	$\mathbf{E_1}$	$\mathbf{E_2}$		$\mathbf{E_j}$		$\mathbf{E_{J-1}}$	$\mathbf{E_J}$
S_1	K_{11}	K_{12}		K_{1j}		$K_{1,J-1}$	K_{1J}
S_2	K_{21}	K_{22}		K_{2j}		$K_{2,J-1}$	K_{2J}
S_i	K_{i1}	K_{i2}		K_{ij}		$K_{i,J-1}$	K_{iJ}
S_{I-1}	$K_{I-1,1}$	$K_{I-1,2}$		$K_{I-1,j}$		$K_{I-1,J-1}$	$K_{I-1,J}$
S_I	K_{I1}	K_{I2}		K_{Ij}			K_{IJ}

$$F_{r,i} = \sum_{l=1}^{l=J} \frac{\left[E_l\right]}{K_{il}}$$

$$\frac{d\left[S_i\right]_{T,j}}{dt} = -\frac{k_{2,ij}^{+}\left[E_j\right]\left[S_i\right]/K_{ij}}{1+F_{c,j}+F_{r,i}}$$

Figure 2. Graph representation of the ECA kinetics as derived in Tang and Riley (2013a). The equation in blue shows the uptake of substrate S_i by consumer E_j as a function the normalized substrate flux $F_{c,j}$ and its conjugate flux $F_{r,i}$. Here subscript "c" designates column, and "r" designates row. When K_{ij} is infinity or a very large number compared to other entries in the matrix, the interaction between substrate S_i and consumer E_j can be ignored.

An example unit block for applying the network-oriented SUPECA kinetics

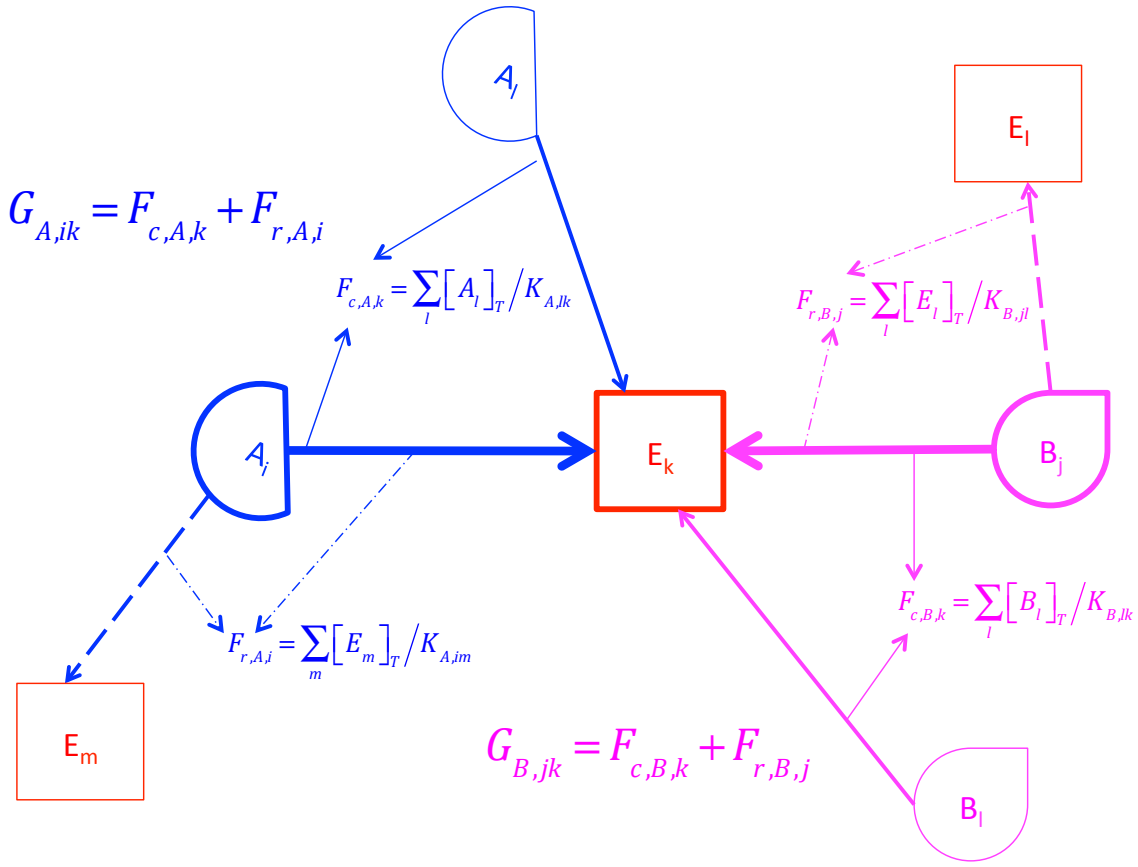

Figure 3. Graph representation for the relationships between substrates, consumers, and normalized fluxes and their conjugates for a block unit of a large substrate-consumer network.

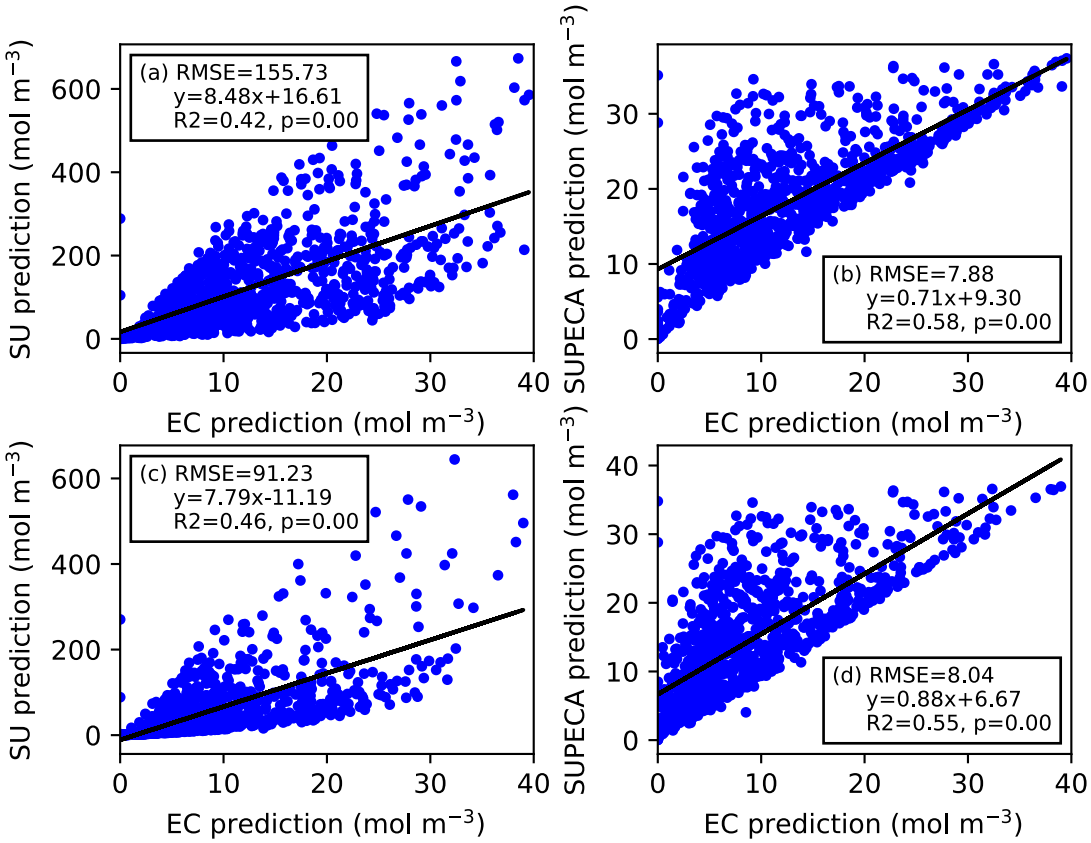

Figure 4. Benchmark of the SU (left column) and SUPECA (right column) predictions against those by the full EC formulation. We note that the y-axes of the left panels are of much larger scale than those on the right. The problem is formulated in Appendix F. Panels (a) and (b) are for the case when $M = 0$; panels (c) and (d) are for uniformly distributed $M > 0$. The related distributions of parameters are in Figure S1 of the supplemental material.

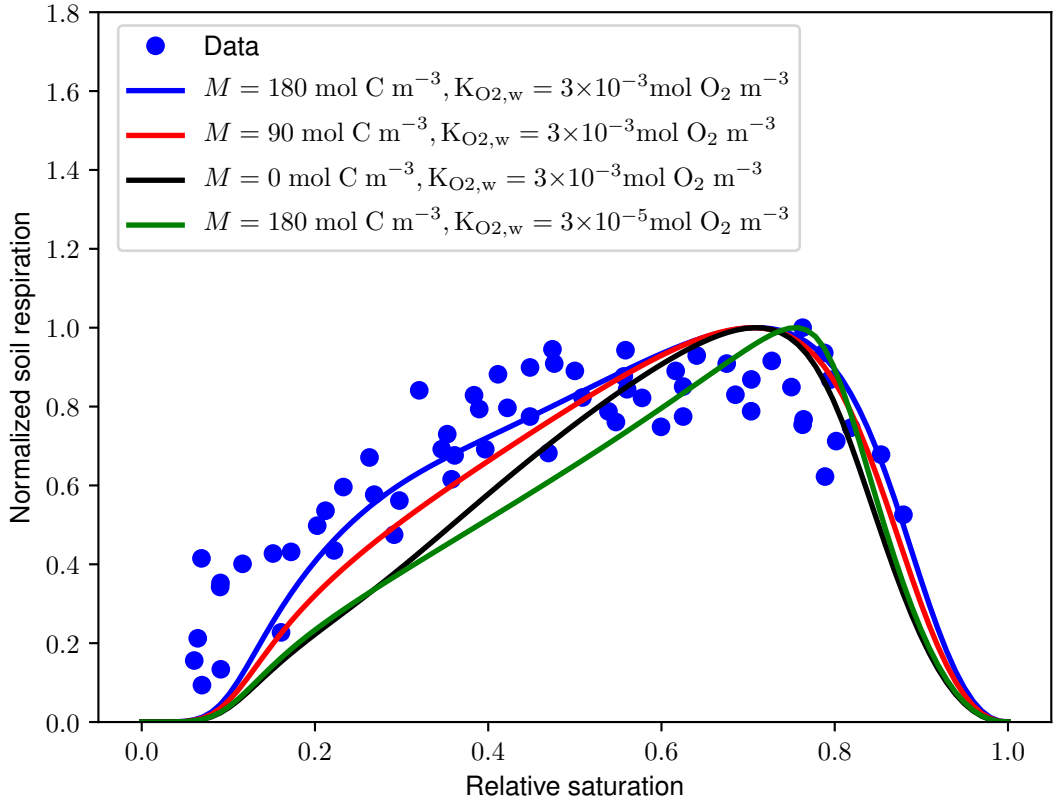

Figure 5. Comparison of predicted normalized soil moisture response functions to that derived from incubation data from Franzluebbers (1999). All response functions are normalized with their respective peak respiration.

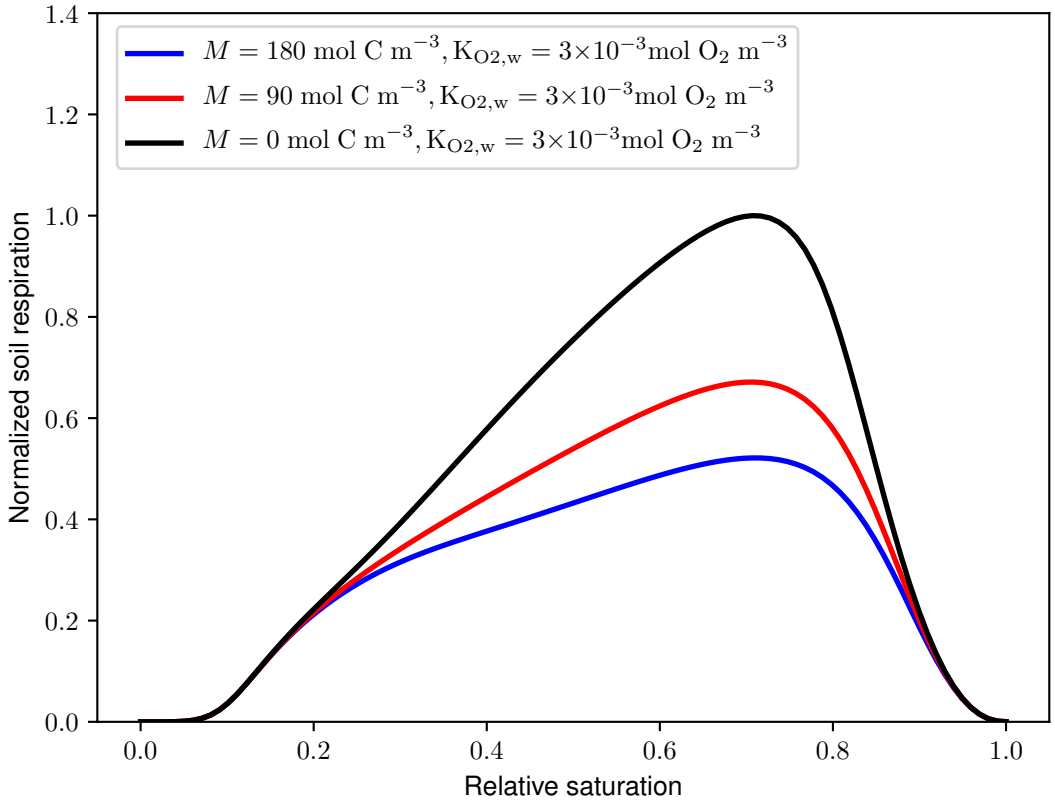

Figure 6. Simulated moisture response functions using elevated affinity parameter for O_2. The respiration data are normalized with the peak value from the case with zero soil minerals (i.e., black line in Figure).

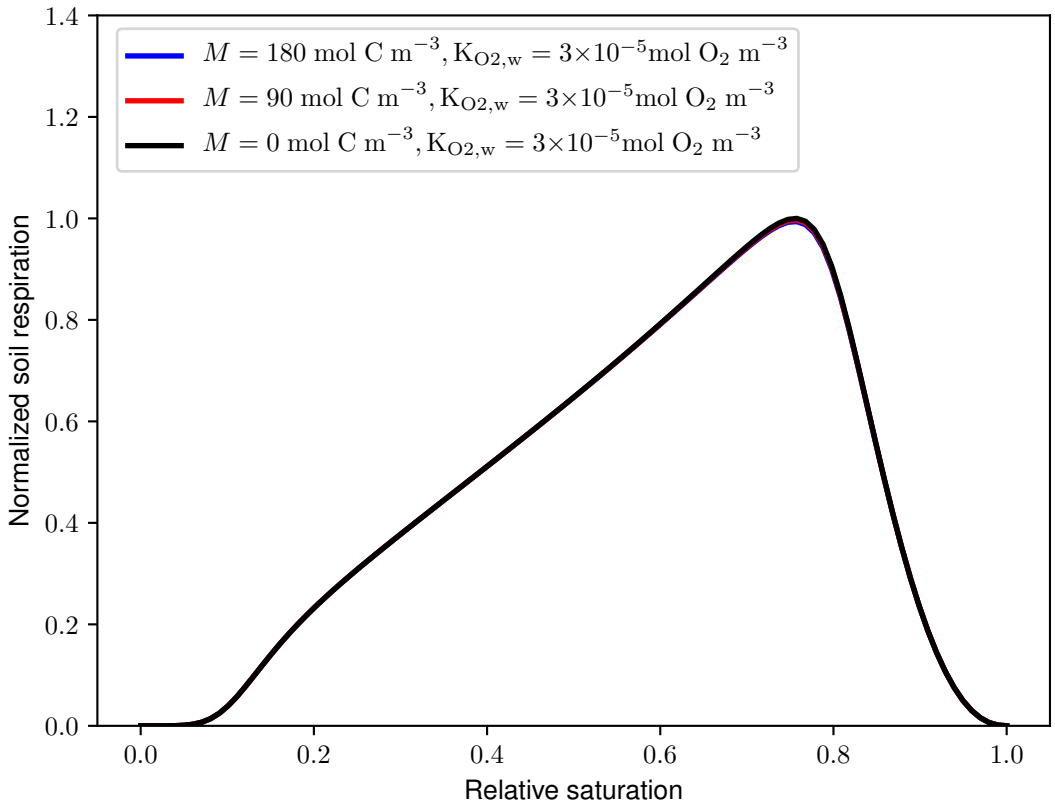

Figure 7. Simulated moisture response functions using default affinity parameter for O_2. The respiration data are normalized with the peak value from the case with zero soil minerals (i.e., black line in Figure). Note here all three lines overlap each other almost perfectly.